Mechanical force of uterine occupation enables large vesicle extrusion from proteostressed maternal neurons

Guoqiang Wang*[,1], Ryan Guasp*[,1], Sangeena Salam*[,1], Edward Chuang[1], Andrés Morera[1], Anna J Smart[1], David Jimenez[1], Sahana Shekhar[1], Ilija Melentijevic[1], Ken C Nguyen[2], David H Hall[2], Barth D Grant[1], Monica Driscoll[1,3]

* Co-first authors
1. Department of Molecular Biology and Biochemistry, Nelson Biological Laboratories, Rutgers, The State University of New Jersey, Piscataway, New Jersey 08854, USA.
2. Department of Neuroscience, Albert Einstein College of Medicine, Bronx, New York 10461, USA.
3. Corresponding to: driscoll@dls.rutgers.edu

Abstract

Large vesicle extrusion from neurons may contribute to spreading pathogenic protein aggregates and promoting inflammatory responses, two mechanisms leading to neurodegenerative disease. Factors that regulate extrusion of large vesicles, such as exophers produced by proteostressed *C. elegans* touch neurons, are poorly understood. Here we document that mechanical force can significantly potentiate exopher extrusion from proteostressed neurons. Exopher production from the *C. elegans* ALMR neuron peaks at adult day 2 or 3, coinciding with the *C. elegans* reproductive peak. Genetic disruption of *C. elegans* germline, sperm, oocytes, or egg/early embryo production can strongly suppress exopher extrusion from the ALMR neurons during the peak period. Conversely, restoring egg production at the late reproductive phase through mating with males or inducing egg retention via genetic interventions that block egg-laying can strongly increase ALMR exopher production. Overall, genetic interventions that promote ALMR exopher production are associated with expanded uterus lengths and genetic interventions that suppress ALMR exopher production are associated with shorter uterus lengths. In addition to the impact of fertilized eggs, ALMR exopher production can be enhanced by filling the uterus with oocytes, dead eggs, or even fluid, supporting that distention consequences, rather than the presence of fertilized eggs, constitute the exopher-inducing stimulus. We conclude that the mechanical force of uterine occupation potentiates exopher extrusion from proximal proteostressed maternal neurons. Our observations draw attention to the potential importance of mechanical signaling in extracellular vesicle production and in aggregate spreading mechanisms, making a case for enhanced attention to mechanobiology in neurodegenerative disease.

INTRODUCTION

In neurodegenerative disease, prions and protein aggregates can transfer among cells of the nervous system to promote pathology spread [1,2]. Determination of the factors that enhance or deter pathological transfer is therefore a central goal in the effort to clinically address neurodegenerative disease. Study of aggregate transfer in the context of the mammalian brain is a major experimental challenge as events are rare, sporadic and transiently apparent, and tissue is not easily accessible for *in vivo* observation. We model aggregate transfer by proteostressed ALMR touch receptor neurons [3-5] in the living *C. elegans* nervous system, an experimental system that enables molecular and genetic manipulation and evaluation in physiological context, directly through the transparent cuticle [6].

More specifically, *C. elegans* adult neurons can extrude large vesicles called exophers (~5µm, 100X larger than exosomes) that carry potentially deleterious proteins and organelles out of the neuron [3-5]. Disrupting proteostasis via diminished chaperone expression, autophagy, proteasome activity, or over-expressing aggregating proteins like human Alzheimer's disease associated fragment $A\beta_{1-42}$, expanded polyglutamine Q128 protein, or high concentration mCherry fluorophore, increases exopher production from the affected neurons. Neurons that express proteotoxic transgenes maintain higher functionality if those neurons produce exophers as compared to those that do not, suggesting that exopher-genesis

can be neuroprotective, at least in young adult neurons. Extruded exopher contents can be transferred to neighboring glial-like hypodermal cell for content degradation in the lysosomal network [7]. Several mammalian models feature similar biology [8-12], and thus we speculate that the basic transfer biology represents a conserved process that can be recruited for animal-wide proteostasis balance.

Neuronal exophers are generated only in adult animals, with an unexpected pattern of a peak at young adult days 2-3 and then later in age with more variable onset [3]. While using chemical regent FuDR to block progeny production for aging studies, we found that blocking reproduction strongly limited the early adult peak of exopher production. Here we report data that support that early adult exopher production is sensitive to the load of eggs in the reproductive tract. We document that uterine expansion, rather than chemical signals emanating from fertilized eggs, correlates strongly with level of exopher production and suggest a model in which mechanical signaling, normally induced across generations from egg to parent via uterine stretch, is a license for proteostressed neurons to release potentially toxic materials in large extracellular vesicles.

Mechanical signaling exerts a profound impact on virtually all cell types, and has been implicated in traumatic brain injury and neurodegenerative disease, yet remains poorly understood [13]. Our observations direct enhanced experimental attention to studies of how mechanical force can influence extracellular vesicle formation and aggregate transfer in living brain and in neurodegenerative disease.

RESULTS

The six *C. elegans* gentle touch receptor neurons (AVM, ALML and ALMR located in the anterior body and PVM, PLML and PLMR located in the posterior body) can be readily visualized *in vivo* by expression of fluorescent proteins under the control of the touch neuron-specific *mec-4* promoter (Fig. 1A). We commonly monitor exophers extruded by the ALMR neuron, which typically produces more exophers than the other touch neurons [3,14], using a strain in which fluorophore mCherry is highly expressed in touch neurons and is avidly eliminated (strain ZB4065 *bzIs166*[$P_{mec\text{-}4}$::mCherry], hereafter referred to as mCherryAg2 for simplicity). ALMR exopher production occurs with a distinctive temporal profile, such that at the L4 larval stage ALMR rarely, if ever, produces an exopher, but in early adult life, the frequency of exopher events increases, typically reaching a peak of 5-20% of ALMR neurons scored at adult day 2 (Ad2); exopher detection then falls to a low baseline level after Ad3 [3,14], a pattern that parallels adult reproduction (Fig. 1B). Late in life, exophers can reappear with variable frequency, but here we focus on young adult exopher generation.

Sterility-inducing drug FUdR suppresses ALMR exophergenesis. In experiments originally designed to study exopher events in aging animals, we sought to generate age-synchronized populations by blocking progeny production from early adult stages using DNA synthesis inhibitor 5-fluoro-2'-deoxyuridine (FUdR). Unexpectedly, we found that 51μM FUdR strongly suppressed exopher events as quantitated at Ad2 (Fig. 1C). FUdR is commonly used in *C. elegans* to inhibit the proliferation of germline stem cells and developing embryos, but has also been noted to impair RNA metabolism [15] and improve adult proteostasis [16]. To probe which FUDR outcome might confer exopher suppression, we first addressed whether disruption of progeny production by alternative genetic means might suppress exophergenesis, which would implicate a viable germline as a factor in exopher modulation.

Germline elimination and germline tumors suppress ALMR exopher production. In the assembly line-like hermaphrodite *C. elegans* gonad, germline stem cells close to the signaling distal tip cell (DTC) proliferate by mitosis (cartoon of *C. elegans* gonad and germ cell development in Fig. 1D). As maturing germ nuclei move through the gonad away from the DTC, nuclei transition to meiosis and enter the pachytene stage in the vicinity of the gonad bend. Germline nuclei transit further through the loop region, exit pachytene, become more fully enclosed by plasma membrane, and form a que of successive maturity states of oocytes in the proximal gonad arm. The most mature oocyte is arrested at meiosis I diakinesis prior to fertilization [17,18]. Somatic gonad, sperm, and oocyte signaling contribute to the maturation of the ovulated oocyte that is primed for fertilization by sperm that are generated earlier in development and stored in the spermatheca [19].

We disrupted germ cell production using the *glp-4(bn2ts)* valyl-tRNA synthetase 1 mutant. At the restrictive temperature (25°C), *glp-4(bn2ts)* causes germ cell arrest during the initial mitotic germ cell divisions, effectively eliminating the germline [20]. We constructed an mCherryAg2; *glp-4(bn2ts)* strain and quantitated ALMR exopher production in animals grown at the restrictive temperature, scoring exophers during early adulthood (Fig. 1E). ALMR neurons in the germline-less *glp-4* mutant produced significantly fewer exophers on Ad1-4 as compared to age- and temperature-matched controls.

Both oogenesis and spermatogenesis are critical for early adult exopher production. Given that lack of functional germ cells impaired neuronal exopher production, we sought to test whether oocytes or sperm might be specifically required for exophergenesis, taking advantage of *C. elegans* genetic reagents available for the manipulation of gamete development.

Oogenesis is required for the peak of early adult exophergenesis. In the *C. elegans* hermaphrodite, the differentiation of germline stem cells begins during the L4 larval stage with spermatogenesis, after which sperm production is shut down and oogenesis begins [21]. Genetic mutants that produce only sperm or only oocytes have been well characterized. To test a mutant that produces sperm but no oocytes, we employed *fem-3(q20ts)*, a temperature sensitive gain-of-function mutant that causes germ cells to exclusively differentiate into sperm [22,23]. We constructed an mCherryAg2; *fem-3(q20ts)* line, reared animals at non-permissive temperature 25°C, and scored ALMR exophers in mutant and control worms during early adulthood. In the sperm-only, oocyte-deficient *fem-3(q20ts)* background, we recorded no exophers over the first five days of adulthood (Fig. 1F). We infer that oocytes must be present for early adult ALMR exopher production and conclude that sperm alone are not sufficient to drive exopher elevation.

Spermatogenesis is required for the peak of early adult exophergenesis. To assess neuronal exopher production in the reciprocal reproductive configuration in which animals have oocytes but no sperm, we disrupted spermatogenesis using two approaches. First, we used a temperature sensitive *fem-1* mutation to produce animals with oocytes but no sperm [24]. We crossed *fem-1(fc17ts)* into the mCherryAg2 strain and examined exopher production from ALMR neurons in hermaphrodites at the restrictive temperature of 25°C. We found that ALMR exopher production in *fem-1(fc17)* mutants was suppressed at 25°C (Fig. 1G).

Second, we used the auxin-inducible degron system (AID [25,26]) to degrade SPE-44, an essential protein required for spermatid differentiation [27,28]. In the AID system, addition of auxin to the culture induces rapid degradation of proteins genetically tagged with a specific auxin-dependent degron sequence. AID targeting of SPE-44-degron is highly effective in disrupting sperm maturation [27]. We treated strain ZB4749 (fxIs1[P_{pie-1}::TIR1::mRuby] zdIs5[P_{mec-4}::GFP]; bzIs166[P_{mec-4}::mCherry]; *spe-44*(fx110[*spe-44*::degron]) with auxin during larval developmental stages to block sperm maturation and then transferred Ad1 animals to NGM plates without auxin, a condition that disrupted sperm maturation but allowed oocyte generation. We find that blocking sperm maturation by targeting SPE-44 for degradation abolished ALMR exopher production (Fig. 1H) even though oogenesis is not significantly impacted [27]. We infer that functional sperm must be present for early adult ALMR exopher production and conclude that the presence of oocytes alone is not sufficient to drive exopher elevation in early adult life.

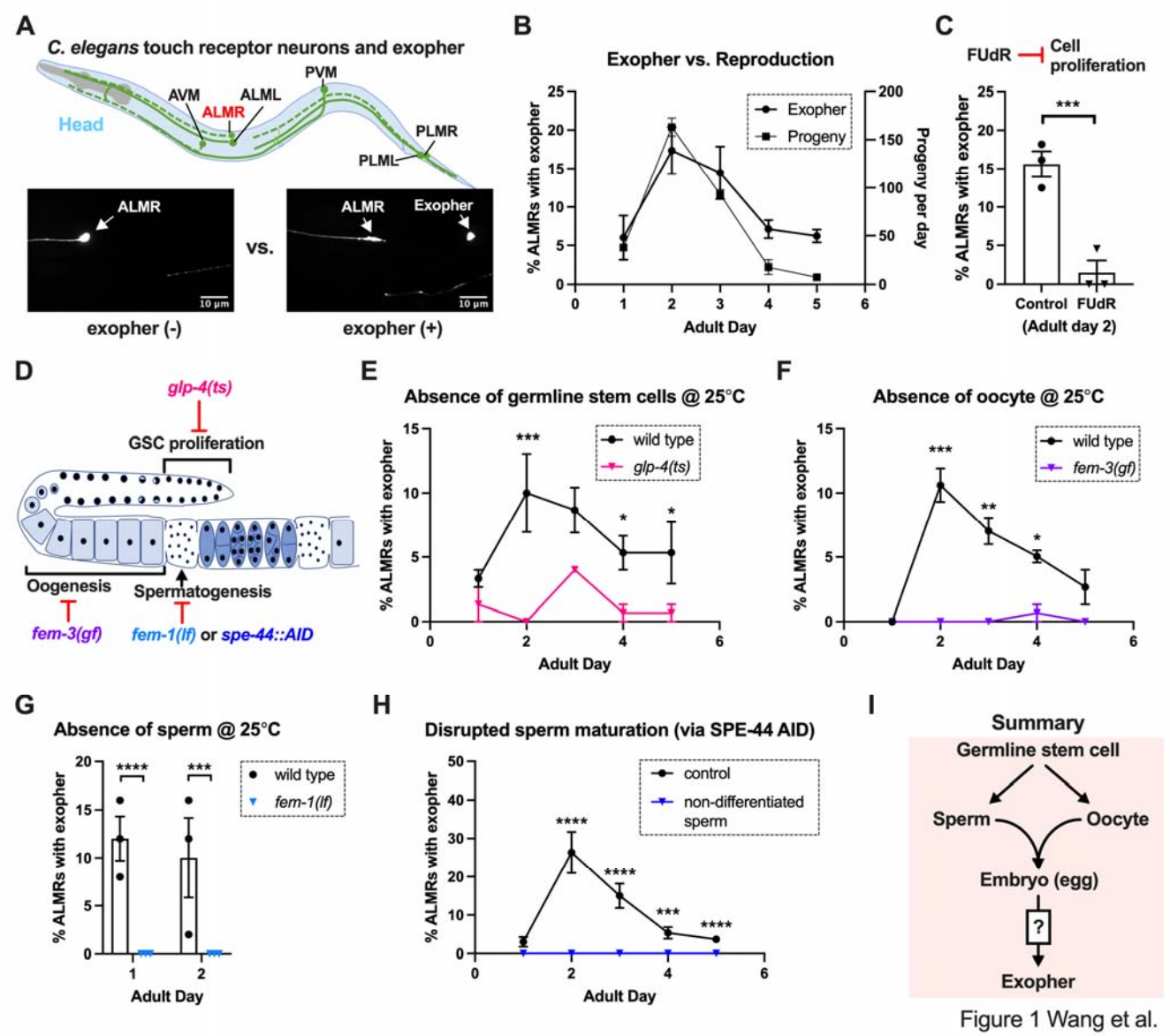

Figure 1. Exophergenesis is dependent on the presence of the germline, ooyctes and sperm.

A. Exophers produced by ALMR are readily visualized in living *C. elegans*. Top, positions of the six *C. elegans* touch receptor neurons: AVM (Anterior Ventral Microtubule cell), ALMR (Anterior Lateral Microtubule cell, Right), ALML (Anterior Lateral Microtubule cell, Left), PVM (Posterior Ventral Microtubule cell, Right), PLMR (Posterior Lateral Microtubule cell, Right) and PLML (Posterior Lateral Microtubule cell, Left). Bottom panels are representative pictures of an ALMR neuron without (lower left) or with (lower right) exopher production from strain ZB4065 *bzIs166*[$P_{mec\text{-}4}$::mCherry], which expresses elevated mCherry in the touch receptor neurons.

B. Both exopher production and reproduction typically peak around Ad2 in the $P_{mec\text{-}4}$::mCherry strain. Left axis: the frequency of exopher events in the adult hermaphrodite *C. elegans* strain ZB4065 at 20°C; Mean ± SEM of 9 independent trials (~50 animals in each trial). Right axis: daily progeny count (Mean ± SEM) from 10 wild type N2 hermaphrodites.

C. FUDR, which inhibits progeny production, suppresses early adult exopher production. Data are the percentage of ALMR exopher events among >50 Ad2 hermaphrodites in each trial (total of 3 independent trials) for strain ZB4065 at 20°C in absence (control) or presence of 51µM FUDR. *** $p < 0.001$ in Cochran–Mantel–Haenszel test.

D. Illustration of the roles of germline development genes tested for impact on exophers. The *C. elegans* reproductive system comprises a biolobed gonad in which germ cells (light blue, dark nuclei) develop into mature oocytes, which are fertilized in the spermatheca (light with sperm indicated as dark dots) and held in the uterus until about the 30 cell gastrulation stage, at which point eggs (dark blue) are laid. Indicated are the steps impaired by germ developmental mutatons we tested.

E. Germline stem cells are required for efficient exopher production. Data show the percentage of ALMR exopher events (Mean ± SEM) among 50 adult hermaphrodite *C. elegans* that express the wild type GLP-4 protein or the GLP-4(ts) protein encoded by *glp-4(bn2)* at 25ºC. All animals express P_{mec-4}mCherryAg2, and the *glp-4(ts*) mutants lack a germline when reared at the restrictive temperature (25ºC). Eggs collected from both wild type and the *glp-4(ts*) mutants were grown at 15ºC for 24 hours before being shifted to 25ºC (at L1 stage) to enable development under restrictive conditions; 3 independent trials of 50 animals represented by each dot; *** $p < 0.001$ or * $p < 0.05$ in Cochran–Mantel–Haenszel test. Note that in WT, temperature shift normally induces a modest elevation in exopher numbers (typically a few % increase, supplemental data in ref. [4]) and is thus not itself a factor in exopher production levels.

F. Oogenesis is required for efficient exopher production. Spermatogenesis occurs but oogenesis is blocked when *fem-3(gf)* mutant hermaphrodites are cultured at 25ºC. Data show the percentage of ALMR exopher events (Mean ± SEM) in hermaphrodite *C. elegans* that express the wild type FEM-3 protein or the temperature-dependent gain-of-function (*gf*) FEM-3 protein (25ºC; 3 independent trials, n=50/trial), *** $p < 0.001$; ** $p < 0.01$ or * $p < 0.05$ in the Cochran–Mantel–Haenszel test.

G. Spermatogenesis is required for efficient exopher production. There is no spermatogenesis in *fem-1(lf)* at the restrictive temperature of 25ºC, while oogenesis is normal in the hermaphrodite. Shown is the percentage of ALMR exopher events (Mean ± SEM) in adult hermaphrodites that express the wild type FEM-1 protein or the temperature-dependent loss of function (*lf*) FEM-1 protein (@25ºC; 3 independent trials, 50 animals/trial). **** $p < 0.0001$ or *** $p < 0.001$ in Cochran–Mantel–Haenszel test.

H. Spermatogenesis is required for efficient exopher production. Data show the percentage of ALMR exopher events (Mean ± SEM) in hermaphrodite *C. elegans* that express the express the SPE-44::degron fusion. SPE-44 is a critical transcription factor for spermatogenesis [28], and is tagged with a degron sequence that enables targeted degradation in the presence of auxin in line ZB4749. In the AID system, auxin is added to the plates in 0.25% ethanol, so “control” is treated with 0.25% ethanol and “no sperm” is treated with 1mM auxin applied to plates in 0.25% ethanol from egg to adult day 1; 4-6 independent trials of 50 animals per trial. **** $p < 0.0001$ or *** $p < 0.001$ in Cochran–Mantel–Haenszel test. Note that under no sperm or non-functional sperm production, oocytes still transit through the spermatheca and enter the uterus; unfertilized oocytes can be laid if the egg laying apparatus is intact.

I. Summary: Genetic interventions that block major steps of germ cell development strongly block ALMR exophergenesis in the adult hermaphrodite. The dual requirement for sperm and oocytes suggests that fertilization and embryogenesis might be required events for inducing ALMR exophergenesis.

Fertilization and early embryonic divisions are required for the early adult exophergenesis peak. The requirement of sperm and oocytes for neuronal exopher production raises the obvious question as to whether fertilized eggs/embryos are required for ALMR exophergenesis (Fig. 1I). *C. elegans* genes impacting fertilization and embryonic development have been studied in exquisite detail [17,18,29,30]. We tested embryonic development genes known for roles at particular stages for impact on neuronal exopher levels using RNAi knockdown approaches.

In *C. elegans* fertilization, as the mature oocyte encounters the sperm-filled spermatheca, a single sperm enters the mature ovulated oocyte (fertilization time 0), triggering the rapid events of egg

activation, which include polyspermy block, eggshell formation, completion of meiotic divisions and extrusion of polar bodies. The multi-step eggshell formation (Fig. 2A) is completed within 5 minutes of sperm entry, by which time the zygote has been passed into the uterus, where the maternal chromosomes execute both meiotic divisions (meiosis accomplished by ~20 minutes after fertilization). After establishment of egg polarity cues, the first mitotic cell division occurs ~40 minutes after fertilization [17,30]. Eggs are held in the mother's uterus until they are laid at the ~30 cell stage (gastrulation). In wild type, ~8 fertilized eggs occupy the uterus when egg laying begins at ~6 hours of adult life [31].

Our data revealed an unexpected theme: we found that disruption of tested early acting genes essential for eggshell assembly (chitin binding domain protein *cbd-1* [32] (Fig. 2B), chitin precursor synthesis gene *gna-2* [33] (Fig. 2C, D), permeability barrier-required CDP-ascarylose synthesis gene *perm-1* [34] (Fig. 2E)) and/or needed for the progression through the 1-cell or 2-cell stages of embryonic development [35-38] (profilin *pfn-1*, coronin-related *pod-1* and cytochrome P450 oxidoreductase *emb-8*) cause potent suppression of ALMR exophergenesis (Fig. 2F). In contrast, RNAi knockdowns of genes essential for the later stage embryonic development (4 cell to 8 cell stages *mex-3*, *mom-2*, gastrulation genes *end-1/-3* or *gad-1)* confer negligible impact on ALMR exophergenesis (Fig. 2G). Our data support a fertilization requirement for neuronal exopher stimulation and suggest that the exophergenesis signal/condition that promotes the early adult wave of exophergenesis is associated with the very earlest stages of embryonic development. Of note, disruption of eggshell biosynthesis has the immediate downstream consequence of disruption of early polarity establishment and first divisions, such that genetic separation of eggshell production from first division proficiency is not possible (*pod-1* and *emb-8* have been reported to also have eggshell deficits [36,38]). We thus conclude that either eggshell integrity or biochemical events associated with the first embryonic cell divisions are required for neuronal exophergenesis.

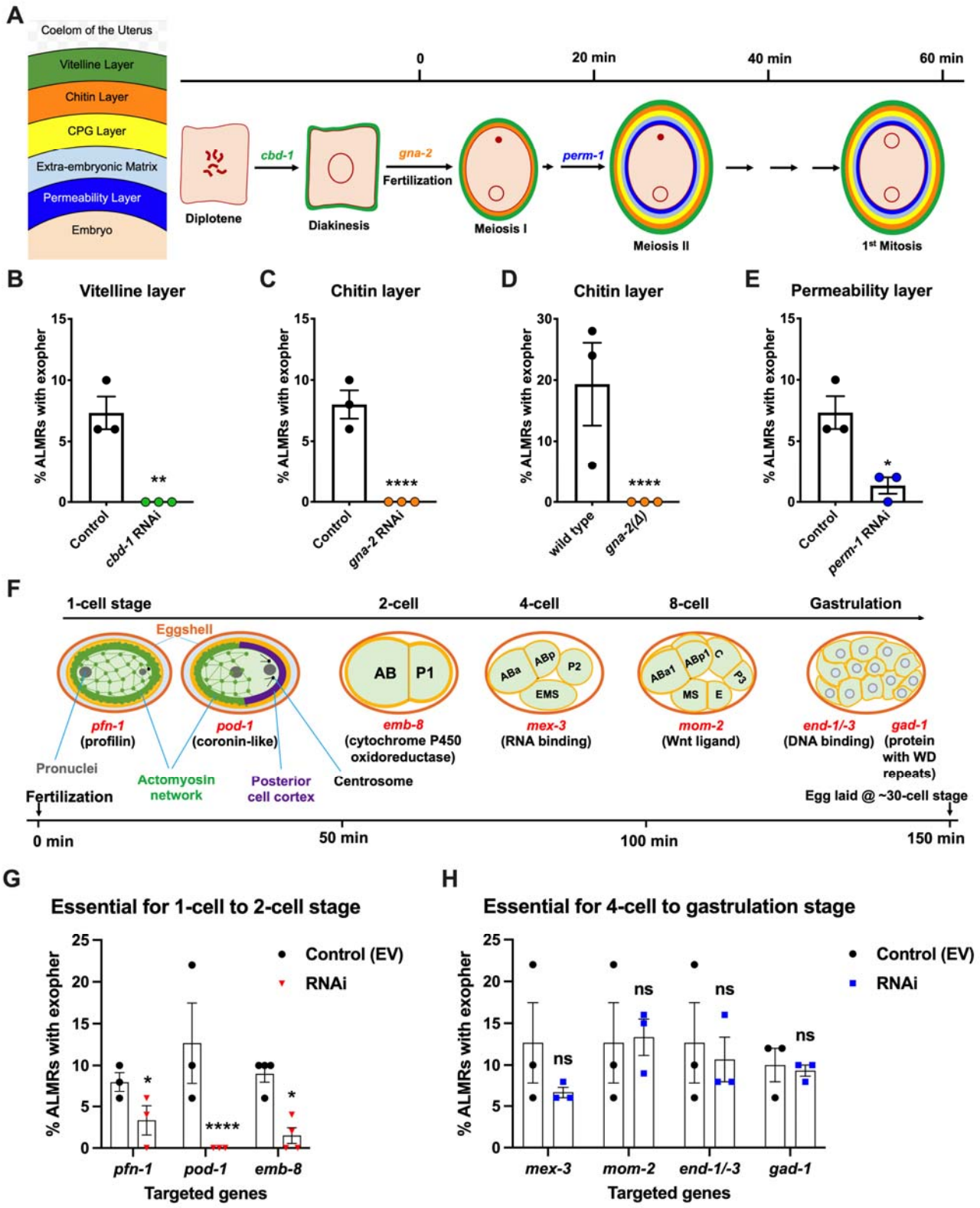

Figure 2: Events required for Ad2 elevation of exopher production occur during the earliest stages consequent to fertilization and are largely completed by the 4 cell stage.

A. Diagram of eggshell layers, post-fertilization timeline for layer formation, and indication of steps at which RNAi disrupts eggshell biogenesis. The formation of the multilayered eggshell is accomplished via a hierarchical assembly process from outside to inside, with outer layers required for later formation of inner layers. The outmost vitelline layer assembles in part prior to fertilization,

dependent on Chitin-Binding Domain protein (CBD-1) [32]. The next eggshell layer is made up of chitin, which confers eggshell stiffness and requires the *gna-2*-encoded enzyme glucosamine-6-phosphate N-acetyltransferase (GNPNAT1) for precursor biosynthesis [33]. The innermost lipid layer of eggshell is called the permeability layer, which is lipid-rich and is needed to maintain osmotic integrity of the embryo. PERM-1 [34] (among others, including FASN-1 [37], POD-1 [36] and EMB-8 [38]) is required for permeability barrier formation [17,39]. Note that eggshell biogenesis is critical for polyspermy barrier, spermathecal exit, meiotic chromosome segregation, polar body extrusion, AP polarization and internalization of membrane and cytoplasmic proteins, and correct first cell divisions [39], so genetic separation of eggshell malformation from the earliest embryonic formation is not possible.

B*. cbd-1*, a gene encoding an essential component of the eggshell vitelline layer, is critical for Ad2 exopher elevation. Exopher scores in Ad2 animals (strain ZB4757: bzIs166[P_{mec-4}::mCherry] II) that were treated with RNAi against *cbd-1*, total of 3 trials (50 hermaphrodites per trial), ** $p < 0.01$ in Cochran–Mantel–Haenszel test, as compared to the empty vector (EV) control.

C, D*. gna-2*, a gene required for chitin precursor biosynthesis and chitin layer formation, is critical for Ad2 exopher elevation. C. Exopher scores in Ad2 animals treated from the L1 stage with RNAi against *gna-2*. The *gna-2* gene encodes enzyme glucosamine-6-phosphate N-acetyltransferase (GNPNAT1) required for chitin precursor biosynthesis.

D. Exopher scores in Ad2 animals harboring a null mutation in the essential *gna-2* gene. *gna(Δ)* homozygous null worms are GFP negative progeny of stain ZB4941: bzIs166[P_{mec-4}::mCherry]; *gna-2(gk308)* I/hT2 [*bli-4(e937) let-?(q782*) qIs48[P_{myo-2}::GFP; P_{pes-10}::GFP; P_{ges-1}::GFP] (I;III). Data represent a total of 3 trials (50 hermaphrodites per trial), **** $p < 0.0001$ in Cochran–Mantel–Haenszel test, as compared to wild type animals.

E. *perm-1*, a gene required for permeability barrier synthesis, is critical for Ad2 exopher elevation. Exopher scores in Ad2 animals treated with RNAi against *perm-1,* which encodes a sugar modification enzyme that acts in the synthesis of CDP-ascarylose. Data represent a total of 3 trials (50 hermaphrodites per trial), * $p < 0.05$ in Cochran–Mantel–Haenszel test, as compared to the empty vector (EV) control. Note that previously characterized strong exopher suppressors *pod-1, emb-8,* and *fasn-1* [4] are also needed for egg shell permeability barrier layer formation [36,38].

F. Diagram of select genes required for specific stages of embryonic development. *pfn-1(RNAi)* (arrest at the one-cell stage [40]); *pod-1(RNAi)* (arrest at the two-cell stage [41]); *emb-8(RNAi)* (arrest at the 1- to 50-cell stage [42]); arrest stage phenotype for other genes is not precisely documented, but these genes play significant roles at the indicated stages; images annotated according to WormAtlas doi:10.3908/wormatlas.4.1).

G. RNAi targeting of early acting embryonic development genes lowers exopher production. Exopher scores from Ad2 animals that were treated with RNAi against genes characterized to be essential for 1-cell to 2-cell stage embryonic development. Total of 3 trials (50 hermaphrodites per trial). * $p < 0.05$ or **** $p < 0.0001$ in Cochran–Mantel–Haenszel test, as compared to the empty vector control. Strong exopher suppressors *pod-1* and *emb-8* have been previously reported [4].

H. RNAi targeting of genes that disrupt 4-cell stage and later embryonic development does not alter exopher production levels. Exopher scores in Ad2 animals that were treated with RNAi against genes that are essential for 4-cell to gastrulation stages of embryonic development. Total of 3 trials (50 hermaphrodites per trial). Ns, not significant in Cochran–Mantel–Haenszel test, as compared to the empty vector control.

Restoring fertilized eggs later in life can extend ALMR exophergenesis. Having found that fertilized eggs are necessary for the early adult elevation in exopher production, we asked whether the presence of eggs is sufficient for stimulation of exopher production by introducing fertilized eggs later in

adult life when they are not normally present. In *C. elegans,* sperm are made in the L4 stage and are stored in the spermatheca to fertilize oocytes that mature in the adult. Sperm are limiting for hermaphrodite self-fertilization, with more oocytes made than can be fertilized by self-derived sperm. Unmated hermaphrodites thus cease egg laying around adult day 4 because they run out of self-supplied sperm. However, if males mate with hermaphrodites, increased progeny numbers can be produced due to increased sperm availability. More germane to our experiment, if males are mated to the reproductively senescing hermaphrodite to replenish sperm, hermaphrodites can produce fertilized eggs for a few additional days (Fig. 3A).

To determine if the presence of eggs might be sufficient to drive exopher production after Ad3, we mated males to Ad3 reproductively senescing hermaphrodites. We found that restored egg production is associated with increased and extended exopher production, provided that hermaphrodites were mated to fertilization-proficient males (Fig. 3B). We conclude that adult ALMR exophergenesis is driven by the presence of fertilized eggs and that the older age decrease in exopher production (~Ad4) under standard culture conditions is more likely attributed to the lack of fertilized egg accumulation at this lifestage, rather than to the existence of a chronological limit on the biochemical capacity to elevate exopher levels at older ages.

Genetically induced egg retention elevates ALMR exopher production. Fertilized eggs might release a signal or create a condition that stimulates exophergenesis. If such an influence was limiting, increasing the egg concentration in the body might increase exopher numbers. To address whether elevating the young adult egg load can increase exophers, we took multiple distinctly-acting genetic approaches to limit egg laying and promote egg retention in the body (Fig. 3C). We tested four genetic conditions that lower or block egg-laying: a null mutation of prolyl hydroxylase *egl-9*, for which disruption induces a mild egg laying defect [43]; a null allele of proprotein convertase subtilisin/kexin type 2 *egl-3* [44] that perturbs neuropeptide processing and confers a severe egg-laying defective phenotype [43]; a reduction-of-function mutation in SOX transcription factor *sem-2(n1343)* that eliminates production of the sex myoblasts needed to generate egg laying muscle; and RNAi directed against the *lin-39* homeobox transcription factor HOXA5 ortholog required for vulval cell fate specification [45,46].

We found that the associated massive egg retention correlated with a dramatic elevation of exopher numbers for each genetic impediment to egg laying (*egl-9* (Fig. 3D); *egl-3* (Fig. 3E); *sem-2* (Fig. 3F), *lin-39*(RNAi) (Fig. 3G)). For example, ~80% of the *sem-2(rf)* mutants produced ALMR exophers on Ad1, compared to only ~6% of WT (Fig. 3F). We conclude that, regardless of the genetic strategy employed to trap eggs in the body, egg retention can lead to high ALMR exopher production.

Hyperactive egg-laying and consequent low egg retention is associated with low exopher production.
Neurotransmitters octopamine (OA) and serotonin (5-HT) have been well documented to play opposite roles in *C. elegans* egg-laying behavior [47]. Feeding *C. elegans* octopamine strongly suppresses egg-laying to induce egg retention, while supplementing with 5-HT causes hyperactive egg-laying [48]. Consistent with outcomes in animals physically blocked for egg-laying, treatment with egg retention-promoting OA enhanced ALMR exophergenesis (Fig. 3H).

To test the outcome of 5-HT-induced enhanced egg laying, we measured the impact of 5-HT consequent to 6 hour food withdrawal, a condition that we previously found markedly enhances ALMR exophergenesis [4], and therefore is expected to increase the dynamic range for scoring exopher suppression. We find that 5-HT treatment, which lowers egg retention, strongly suppresses fasting-associated ALMR exophergenesis (Fig. 3H). Although perturbing neuronal signaling holds complex consequences for whole-animal physiology, our findings are consistent with a model in which high egg load increases neuronal exophergenesis, and low egg retention decreases exophergenesis.

The egg laying circuit is controlled in part by Goα inhibition--null allele *goa-1(n1134)* removes this inhibition such that eggs are often laid at very early developmental stages (2-4 cell stage) rather than being retained in the uterus until gastrulation (~30 cell stage) [49]. We introduced *goa-1(n1134)* into the

mCherryAg2 background and scored ALMR exopher events at Ad2. We confirmed that *goa-1(n1134)* retains few eggs in the uterus and is associated with a significantly lower number of ALMR exopher events as compared to the age-matched wild type control (Fig. 3I).

In sum, manipulation of uterine egg occupancy is strongly correlated with the extent of ALMR neuronal exophergenesis—high egg retention promotes high exophergenesis and low egg retention is associated with exophergenesis block.

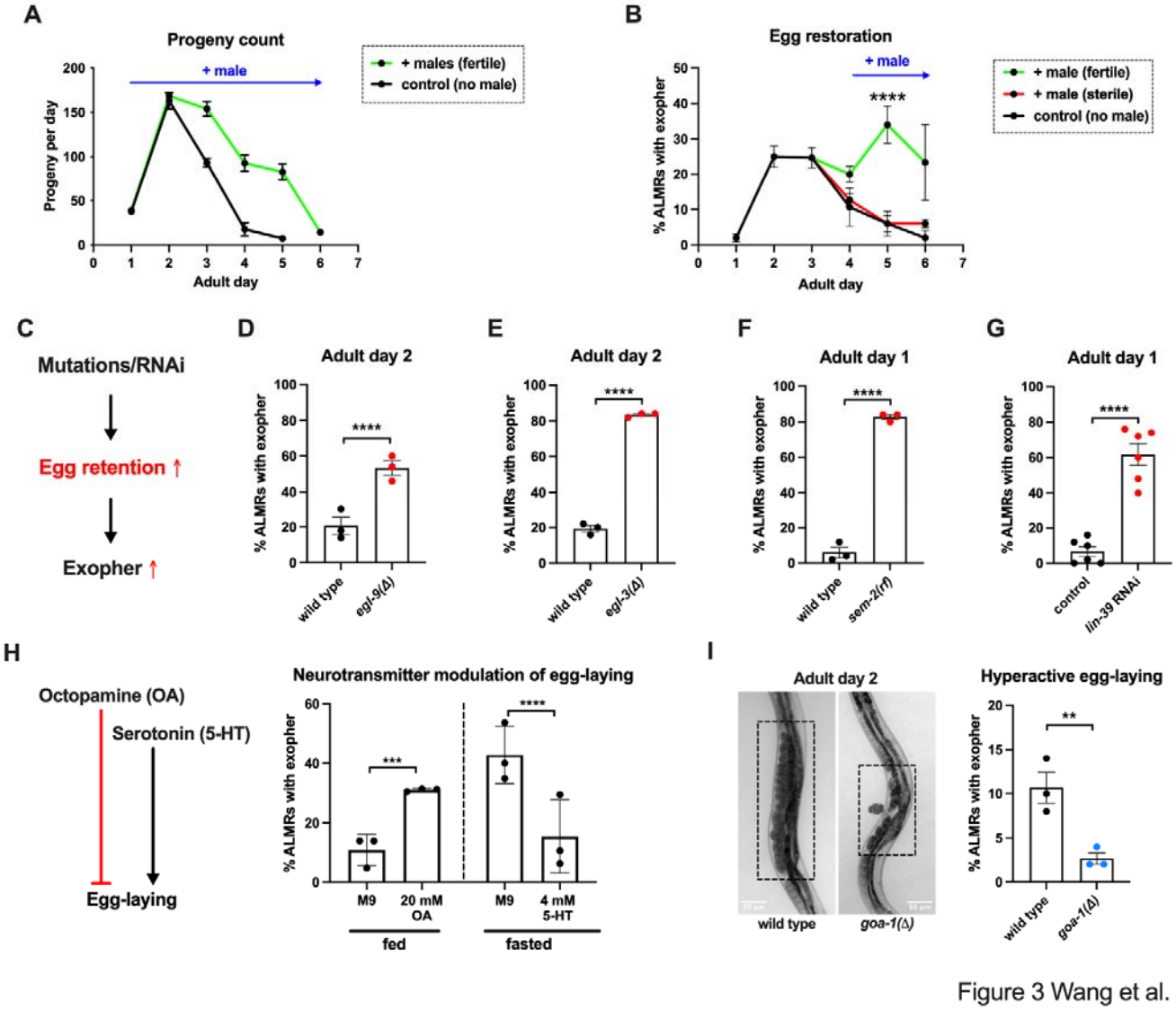

Figure 3 Wang et al.

Figure 3: ALMR exophergenesis levels are markedly influenced by the number of fertilized eggs retained in the uterus.

A. Later life mating extends the *C. elegans* reproductive period. Progeny count for each wild type hermaphrodite in the presence (green) or absence (black) of males (1 hermaphrodite +/- 5 males) from Ad1 to Ad6. Total of 10 wild type hermaphrodites scored for each condition. Data shown are mean ± SEM.

B. Introducing fertilized eggs in late adulthood extends the period of elevated exophergenesis. Males carrying functional (green) or nonfunctional (red) sperm (*spe-45(tm3715)*) were added to plates housing hermaphrodites as endogenous stores of sperm are depleted at Ad3. Data shown are mean ± SEM of percentage hermaphrodite ALMR neurons exhibiting an exopher event on days indicated. Total of 3 trials, and 50 hermaphrodites for each treatment at a single time point. **** $p < 0.0001$ in Cochran–Mantel–Haenszel test, as compared to the sterile male group or no male control.

C. Hypothesis: Genetic interventions (mutations/RNAi) that increase egg retention will increase ALMR exophergenesis.

D-G. Genetic interventions that induce egg retention elevate exopher levels. All data are a total of three trials (50 worms per trial, each trial one dot); **** $p < 0.0001$ in Cochran–Mantel–Haenszel test, as compared to the wild type control.

D. *egl-9(sa307).* ALMR exopher scores Ad2. Strain ZB4757: bzIs166[P_{mec-4}::mCherry] II vs. strain ZB4772: bzIs166[P_{mec-4}::mCherry] II; *egl-9(sa307)* V.

E. *egl-3(gk238).* ALMR exopher scores Ad1. Strain ZB4757: bzIs166[P_{mec-4}::mCherry] II vs. strain ZB4904: bzIs166[P_{mec-4}::mCherry] II; *egl-3(gk238)* V. Exophers were scored in control and RNAi on Ad1 because of the damaging excessive bagging that ensues in this background.

F. *sem-2(n1343).* ALMR exopher scores Ad1. Strain ZB4757: bzIs166[P_{mec-4}::mCherry] II vs. strain ZB4902: *sem-2(n1343)* I; bzIs166[P_{mec-4}::::mCherry] II. Exophers were scored in control and RNAi on Ad1 because of the damaging excessive bagging that ensues in this background.

G. *lin-39(RNAi)*. ALMR exopher scores Ad2. Strain ZB4757: bzIs166[P_{mec-4}::mCherry] II treated with RNAi against *lin-39*.

H. Egg-laying modulating neurotransmitters octopamine (OA) and serotonin (5-HT) influence ALMR exophergenesis levels. Data show the mean ± SEM of percentage hermaphrodite ALMR neurons exhibiting an exopher event at Ad2 after 48 hours of treatment with 20mM octopamine (OA) or 4mM serotonin (5-HT) on OP50 bacteria seeded NGM plates. Because 5-HT (which increases egg laying) was hypothesized to suppress exopher production, we assayed under conditions of six hour food limitation, which markedly raises the exopher production baseline, enabling easier quantiation of suppression effects [4]. Total of 3 trials and 50 hermaphrodites per trial for each condition. *** $p < 0.001$ or **** $p < 0.0001$ in Cochran–Mantel–Haenszel test, as compared to the control group treated with M9 buffer (solvent for OA or 5-HT).

I. Mutant *goa-1(n1134),* with hyperactive egg-laying and low egg retention in the uterus (pictures on the left, representative of 20), has low exopher scores at Ad2. Strain ZB4757: bzIs166[P_{mec-4}::mCherry] II vs. strain ZB5352: *goa-1(n1134)* I; bzIs166[P_{mec-4}::mCherry] II. Boxes highlight egg zone. **p< 0.01.

ALMR neuron proximity to the egg zone correlates with exophergenesis frequency. The ALML and ALMR anterior touch neurons share developmental, morphological and functional similarities [50], yet paradoxically, ALMR consistently produces exophers at higher levels than ALML [3] (also Fig. 4G). The ALM neurons are embedded within the *C. elegans* hypodermis, but the ALMR soma is situated in vicinity of the gonad and its resident eggs, whereas the ALML soma, on the opposite side of the animal, is positioned closer to the intestine (Fig. 4A, 4B) [51].

To ask if proximity to the gonad is correlated with exopher production, we randomly selected 128 Ad2 hermaphrodites that expressed mCherry in the touch receptor neurons, imaged in brightfield to visualize the egg zone of each animal, and imaged again in the red channel to visualize the touch neuron, recording the relative positions of ALMR and the egg zone (Fig. 4C). We also assessed whether the ALMR neuron had produced an exopher or not.

We found that 37/128 ALMRs examined had produced an exopher (Exopher+), and that 36/37 (95%) of the ALMR neuronal somas that had produced exophers were positioned within the visualized egg zone (Fig. 4D). For the ALMRs that had not produced exophers, fewer (63/91; 70%) ALMR neurons were

located in the egg zone ($p < 0.01$ in Chi-Square test, Fig. 4D), a first indication that proximity of ALMR to eggs is associated with higher exopher frequency.

To further test for association of egg zone proximity to ALMR and exopher production, we genetically shifted ALM position. During development, the ALM neurons migrate posteriorly to near the mid-body [52] and most commonly, ALM somas are situated posterior to AVM. ALM soma positions, however, can be influenced by migration and specification cues. In particular, transgenic introduction of a *mec-3* promoter fragment bearing an internal deletion (fusion of the -1 to -563 sequences to the -1898 to -2372 *mec-3* promoter fragment, plasmid pJC4) can induce anterior ALM migration during development, sometimes resulting in final ALM positions anterior to AVM [53] (Fig. 4E). We took advantage of the partially deleted *mec-3* promotor sequences in pJC4 to manipulate ALM position. In these studies we introduced pJC4 with the co-transformation marker pRF4 (*rol-6(su1006))* that disrupts the cuticle to induce rolling of transgenic animals into the $P_{mec\text{-}4}$::mCherry background. Rol hermaphrodites have a strikingly high baseline of ALMR exophergenesis (~71% exophers in rollers vs. ~20% in the wild type) (Fig. 4F). Strikingly, we found that when ALMs are situated anterior to AVM, ALMR exophergenesis drops to ~5% (4/73) vs. 71% for posterior position (55/78) (Fig. 4F). Although we cannot exclude that physiological changes in differently-positioned touch neurons underlie reduced exophergenesis, data are consistent with a model in which proximity to the egg zone correlates with exophergenesis.

Another way to increase egg proximity to ALMR is to disrupt egg laying capacity, which confers egg retention and uterine expansion. We hypothesized that in the *sem-2(rf)* mutant, which is associated with considerable internal egg accumulation, additional touch neurons should experience increased proximity to eggs in the blocked uterus. Indeed, we find that in the *sem-2(rf)* background, every touch neuron that is positioned in the general region of the expanded uterus (ALML, AVM, PVM) increases exopher production, but the posterior PLM neurons, which cannot be approached by the gonad, do not produce exophers (Fig. 4G). Thus, touch neurons can be stimulated to produce exophers if the egg domain is artificially brought closer to them. Data are consistent with a model in which ALMR normally makes most exophers because of its closest natural positioning near the egg-filled uterus. Possibilities are that a diffusible signal may eminate from the filled uterus or that mechanical pressure associated with a filled uterus might signal enhanced exophergenesis.

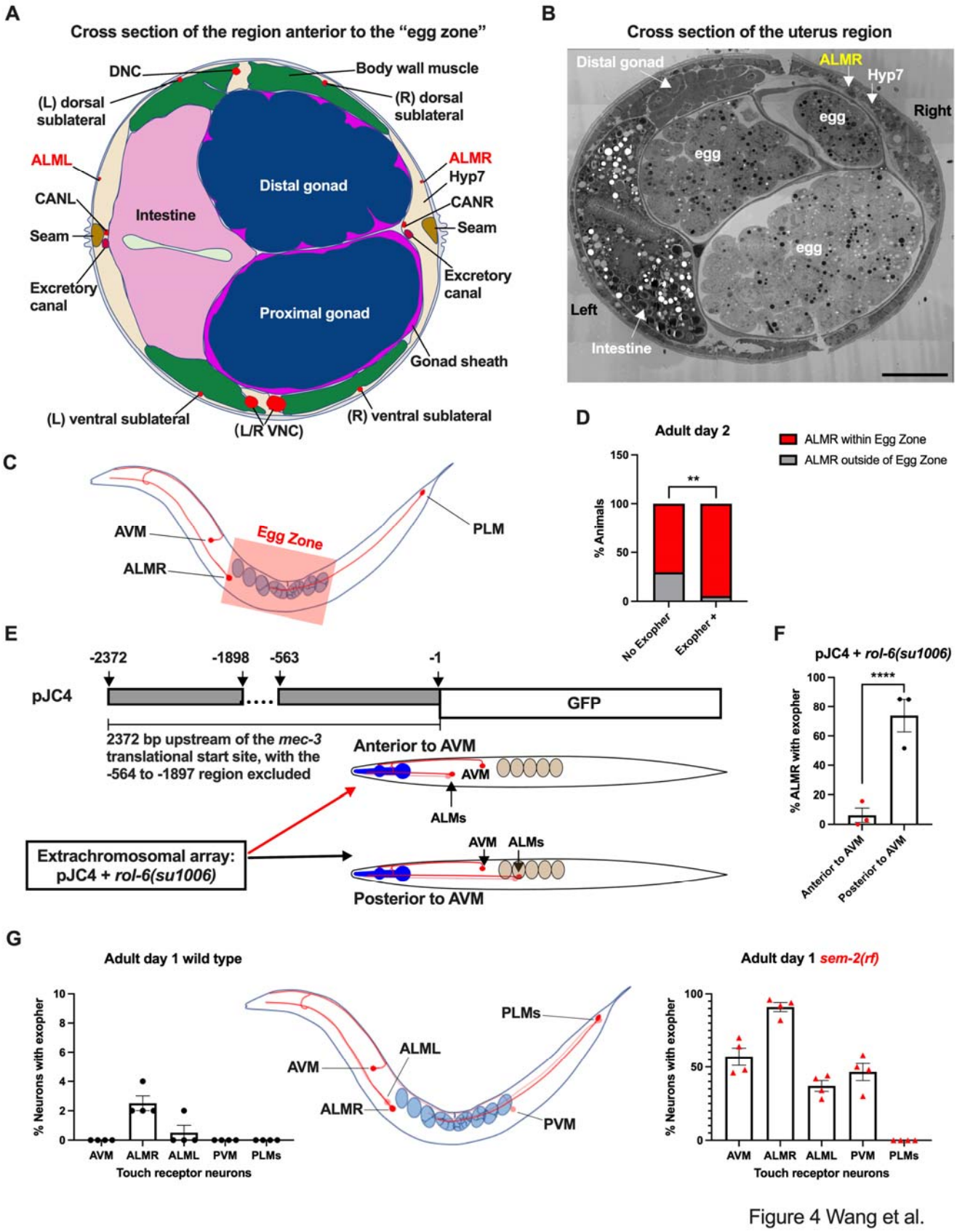

Figure 4. ALMR exophergenesis levels correlate with proximity to the egg zone.

A,B. ALMR is positioned close to the uterus and ALML is situated on the opposite side, close to the intestine.

A. A diagram of ALMR and ALML positions relative to major body organs in cross section that is anterior to the "egg zone". Image drawing based on the EM pictures of adult hermaphrodite slice #273 of WormAtlas. DNC: dorsal nerve cord; VNC: ventral nerve cord; Hyp7: hypodermal cell 7; CAN(L/R): canal associated neurons (left/right); neurons in red.

B. Electron microscopy cross section image of the uterus region indicating ALMR soma and eggs within the adult uterus. Note ALMR is close to the egg-filled uterus, ALML is on the opposite side closer to the intestine. The ALML soma is not evident in this cross section.

C. Illustration of the egg zone definition, distance between outermost eggs. The measure of this distance corresponds to uterine length.

D. ALMRs positioned close to the filled gonad produce exophers more frequently than ALMRs that are positioned a bit more distally. We selected Ad2 mCherry animals at random, then identified whether or not ALMR had produced an exopher, and subsequently determined whether ALMR was positioned within the egg zone or outside the egg zone as indicated (neuronal soma positioning differences are a consequence of developmental variation). Neurons with somas positioned further from the egg area produced fewer exophers than neurons within the egg zone indicated; total of 91 worms for the "No Exopher" group and 37 for the "Exopher +" group; ** $p < 0.01$ in Chi-Square test.

E, F. ALMR neurons genetically induced to adopt positions further away from the uterus generate fewer exophers then those close to the uterus. The Aamodt group [53] previously reported that high copy numbers of plasmid pJC4 containing the *mec-3* promoter region (-1 to -563, and -1898 to -2372 of the *mec-3* translational start) exhibited increased abnormal positioning of ALM neurons anterior to AVM. We introduced plasmid pJC4 along with transformation reporter pRF4 *rol-6(su1006)* in the background of mCherryAg2 (note this revealed that *rol-6(su1006)* is a strong exopher enhancer) and identified neurons that were positioned posterior to AVM (normal, close to the uterus) and those that were positioned anterior to AVM (further away from the uterus). **B**. We counted numbers of exophers produced in Ad2 Rol hermaphrodites for each position type. Strain ZB5046: Ex [(pJC4) P_{mec-3}::GFP + pRF4]; bzIs166[P_{mec-4}::mCherry] II. Total of three trials (61 (34a + 27p); 39(19a + 20p); 51(20a + 31p) animals per trial); **** $p < 0.0001$ in Cochran–Mantel–Haenszel test.

G. When eggs cannot be laid in the *sem-2(rf)* mutant, the eggs that accumulate in the body are brought in closer proximity to ALML, AVM and PVM touch neurons with a resulting increase in their exopher production. Strain ZB4757: bzIs166[P_{mec-4}::mCherry] II vs. strain ZB4902: *sem-2(n1343)* I; bzIs166[P_{mec-4}::mCherry] II. Left, Exopher scoring (Mean ± SEM) of all six touch receptor neurons in Ad1 wild type hermaphrodite; Right, Exopher scoring (Mean ± SEM) of all six touch receptor neurons in Ad1 *sem-2(rf)* hermaphrodite. Total of 4 trials (50 worms per trial) for each. Wild type, egg laying proficieint animals on Ad1 exhibit low exopher levels, but when eggs accumulate early in the *sem-2* mutant, exophers markedly increase in ALMR and other touch neurons that are in the vicinity of an expanded uterus. PLM neurons are situated posterior to the anus and are not subject to uterine squeezing effects.

Uterine expansion associated with high egg load correlates with high exophergenesis. How might the presence of eggs signal to the maternal neurons to induce exophers? We consider two main possibilities: 1) eggs filling the uterus might exert physical pressure that activates essential stretch-signaling for young adult neuronal exopher release. This mechanical stretch signal might act directly (for example introducing chronic and/or dynamic pressure on the touch neurons), or indirectly (possibly inducing the stretched uterus/somatic gonad to release chemical signals that promote neuronal exopher formation); 2) early fertilized eggs might release a short-range chemical signal that contributes to young adult proteostasis reorganization [54,55] to promote exophergenesis.

To begin to dissect the role of egg pressure in promoting exophergenesis, we analysed the physical relationships of neurons, eggs and uterine shape. Eggs can readily be observed to distort tissue structure in young adult *C. elegans*. For example, in a strain that expresses GFP to label the hypodermis and expresses mCherry to label the touch neurons, the distortion of the hypodermis by eggs can be easily visualized as dark non-fluorescent eggs project through the observation plane of the hypodermis (Fig. 5A). Thus, the uterus can approach and pressure surrounding tissue, including touch neurons.

We quantitated uterine length as an indicator for stretch in relation to exopher production levels under representative condition of high and low exophergenesis. We found that egg retention mutants that exhibit high exophergenesis, *egl-3(Δ)* (Fig. 5B), *egl-9(Δ)* (Fig. 5C), and *sem-2(rf)* (Fig. 5D), had significantly longer egg zones (*i.e.,* uterus length) as compared to wild type. In contrast, *cbd-1(RNAi)* (Fig. 5E), sperm-less induction with SPE-44 AID (Fig. 5F), and hyperactive egg-laying mutant *goa-1(Δ)* (Fig. 5G), which we find to be strong exophergenesis suppressors, are all associated with short uterine egg zones. The gastrulation mutant *gad-1*, which is not associated with egg retention or exopher elevation, does not have an extended egg zone/uterine length (Fig. 5H), so not all developmental compromises are associated with uterine extension.

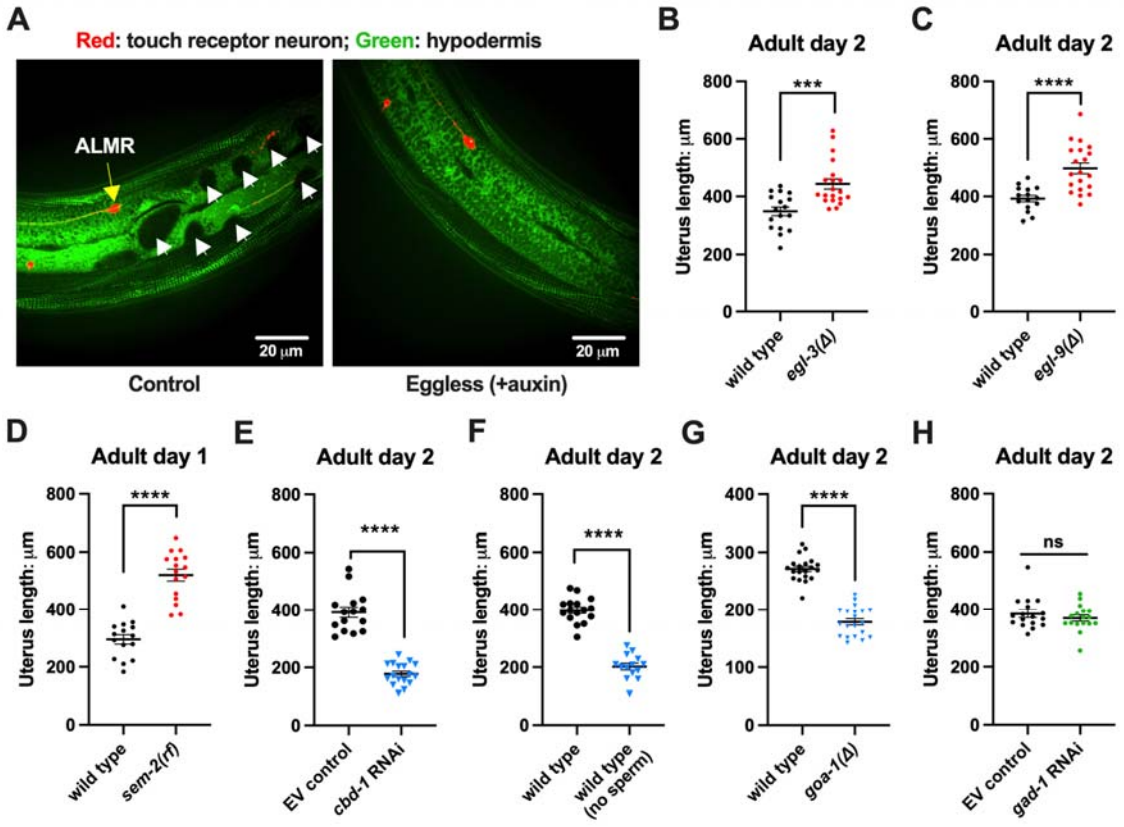

Figure 5 Wang et al.

Figure 5. Uterine length measures for egg-laying defective and gastrulation defective mutants support the correlation of high exopher production and uterine expansion

- **A. Eggs can distort tissues in their vicinity.** Shown is strain ZB4942: fxIs1[Ppie-1::TIR1::mRuby] I; bzIs166[P_{mec-4}::mCherry] II; *spe-44*(fx110[*spe-44*::degron]) IV; pwSi93[Phyp7::oxGFP::*lgg-1*], with touch neurons expressing mCherry (red); and the hypodermis expressing GFP. Dark round areas (white arrows) are eggs that press into the hypodermis when viewed in this focal plane. On the right, slit-like dark regions correspond to hypodermal seam cells.
- **B.** Uterus length of WT vs. *egl-3(Δ);* strain ZB4757: bzIs166[P_{mec-4}::mCherry] II vs. ZB4904: bzIs166[P_{mec-4}::mCherry] II; *egl-3(gk238)* V. n = ~20 hermaphrodites from one trial. *** $p < 0.001$ in two-tailed *t* test.
- **C.** Uterus length of WT vs. *egl-9(Δ)* ZB4757: bzIs166[P_{mec-4}::mCherry] II vs. ZB4772: bzIs166[P_{mec-4}::mCherry] II; *egl-9(sa307)* V. n = ~20 hermaphrodites from one trial. **** $p < 0.0001$ in two-tailed *t* test.
- **D.** Uterus length of WT vs. *sem-2(rf);* strain ZB4757: bzIs166[P_{mec-4}::mCherry] II vs. ZB4902: *sem-2(n1343)* I; bzIs166[P_{mec-4}::mCherry] II. n = ~20 hermaphrodites from one trial. **** $p < 0.0001$ in two-tailed *t* test.
- **E. Uterine length is short under *cbd-1(RNAi)* compared to WT + empty vector RNAi.** Uterus length of strain ZB4757: bzIs166[P_{mec-4}::mCherry] treated with RNAi against *cbd-1* or control empty vector feeding RNAi. n = ~20 hermaphrodites from one trial. **** $p < 0.0001$ in two-tailed *t* test.
- **F. When sperm maturation is blocked in egg laying competent animals, leaving oocytes to occupy reproductive structures, the uterus length is short**. Uterus length of strain ZB4749: fxIs1[P_{pie-1}::TIR1::mRuby] zdIs5[P_{mec-4}::GFP] I; bzIs166[P_{mec-4}::mCherry1] II; *spe-44(fx110[spe-44::degron]*) IV. 1 mM auxin treatment induces the no sperm status. n = ~20 hermaphrodites from one trial. **** $p < 0.0001$ in two-tailed *t* test.
- **G. Uterine length is short in the hyperactive egg-laying mutant which has low occupancy of eggs in the uterus**. Uterus length of strain N2: wild type vs. strain MT2426: *goa-1(n1134)* I. n = 20 hermaphrodites from one trial. **** $p < 0.0001$ in two-tailed *t* test.
- **H. Gastrulation defective mutant *gad-1* has normal uterine length.** Uterus length of strain ZB4757: bzIs166[P_{mec-4}::mCherry] treated with RNAi against the *gad-1* gene. *gad-1* disrupts gastrulation at the stage at which eggs are normally laid and perturbs later development but not egg shell formation and egg laying. n = ~20 hermaphrodites from one trial. Not significant (ns) in two-tailed *t* test as compared to the empty vector control.

Even when eggshell production and early embryonic divisions are disrupted, forced uterine expansion can elevate exopher levels. Our initial studies suggest extended uterine length is correlated with high exopher levels, but high egg retention is also a feature of an extended uterus. To begin test a requirement for fertilized eggs *per se* in the exopher influence, we asked whether egg viability is essential for promoting early adult exophergenesis. We manipulated egg integrity/uterine contents in egg retention mutants by egg/embryo perturbation, testing for impact on exophergenesis.

Under conditions of *cbd-1(RNAi)*, eggshell development and embryonic development are blocked; eggs that form are fragile and can be malformed consequent to passing through the spermatheca into the uterus; embryonic development does not proceed and egg remnants tend to be sticky [56]. As shown in Fig. 2B (and again in Fig. 6A), treating WT reproductive animals (that have functional egg laying capacity) with *cbd-1*(RNAi) to kill embryos exerts a potent block on ALMR exophergenesis. We proceeded to test the consequence of *cbd-1(RNAi)* in mutants that cannot extrude eggs or their remnants, and therefore would retain defective eggshell/dead embryos in the uterus.

We subjected the *sem-2(rf)* egg-laying defective mutant to *cbd-1(RNAi)* so that the uterus would fill with eggshell/dead embryo remains. Strikingly, we found that *cbd-1(RNAi)*/dead embryo retention in the

sem-2(rf) background is still associated with significantly elevated levels of ALMR exophergenesis (~45%), while in egg-laying proficient wild type, barely any ALMR exophergenesis is observed under *cbd-1(RNAi)* conditions (<1%) (69/150 for *sem-2* egg-laying blocked *cbd-1(RNAi)* vs. 1/150 for egg-laying proficient *cbd-1(RNAi)*, Fig. 6A).

Importantly, under conditions of defective eggshell/dead embryo retention associated with *cbd-1(RNAi); sem-2(rf*), the uterine egg zone is expanded (Fig. 6B), extending the correlation of exopher production with uterine length. We conclude that intact eggshells and earliest embryonic divisions are not required for the boost in exopher production observed when uterine contents are forced to accumulate--uterine retention of dead eggs and egg remnants is sufficient for exopher elevation if the egg laying apparatus is defective. Expansion of the uterine compartment, rather than eggshell/embryo integrity, tracks with exopher elevation.

Forced uterine expansion via oocyte accumulation can elevate exopher levels. Although uterine retention of malformed inviable embryos is sufficient to elevate neuronal exophers when egg laying is blocked, the defective *cbd-1* embryos or debris might still release egg-associated chemical signals. To test for a requirement of any fertilization-dependent egg signals in the egg-laying compromised mutants, we asked whether uterine filling with only oocytes can suffice to promote neuronal exopher elevation. Unfertilized oocytes cannot initiate embryonic development or egg-shell biosynthesis; nor can oocytes elevate ALMR exophergenesis in hermaphrodites that are proficient at egg-laying (Fig. 1G&H).

We tested two distinct uterine retention conditions--*sem-2(rf)* and *lin-39(RNAi*)--in which we used the auxin inducible degron system to disrupt sperm maturation such that only oocytes filled the gonad. For both genetic retention strategies, we found that build-up of retained oocytes in egg-laying blocked animals was sufficient to elevate exophers (Fig. 6C&E) and expand the uterus (Fig. 6D&F). Strikingly, ALMR exophergenesis can occur in approximately 80% (129/150) ALMR upon oocyte retention in the *sem-2(rf)* mutant, which is comparable to the fertilization-proficient, but egg retaining *sem-2(rf)* mutant (Fig. 6A). We conclude that fertilization, egg shells and egg remnants are not essential for the early adult exopher peak. Expansion of the uterus with unfertilized oocytes can suffice to elevate neuronal exopher formation.

Lack of a functional egg-laying apparatus does not induce exopher elevation when the uterus is not filled. The above-described experiments left open the possibility that the lack of a functional egg-laying apparatus itself might be causative in the elevation of exopher production. To address this possibility, we compared disruption of sperm (permissive for oocyte accumulation) to disruption of oogenesis (effectively empties the uterus) when egg-laying capacity was compromised by *lin-39(RNAi)* (Fig. 6G). *lin-39(RNAi)* + oocyte retention promotes exopher formation, but eliminating oocytes (*fem-3(gf)*) eliminates exopher elevation even when egg-laying is blocked by *lin-39(RNAi)* That is to say, although oocyte accumulation with uterine expansion suffices to elevate exophers, removing the oocytes and uterus occupancy eliminates the exopher boost. We observe the same outcome of suppressed exopher formation when *cbd-1(RNAi)*-induced dead embryo retention in the *sem-2(rf)* egg-laying defective mutant (which is exopher inducing) is prevented from oocyte production by *fem-3(gf)* (Fig. 6H). Thus, disruption of egg laying on its own is not the driving factor in high exophergenesis; rather, uterine filling is required.

We revisited the relationship of uterine length and exopher level by adding data from the studies with oocyte retention to reinforce the conclusion that ALMR exophergenesis is strongly correlated with the level of uterus stretching caused by the accumulation of uterine contents (Fig. 6I).

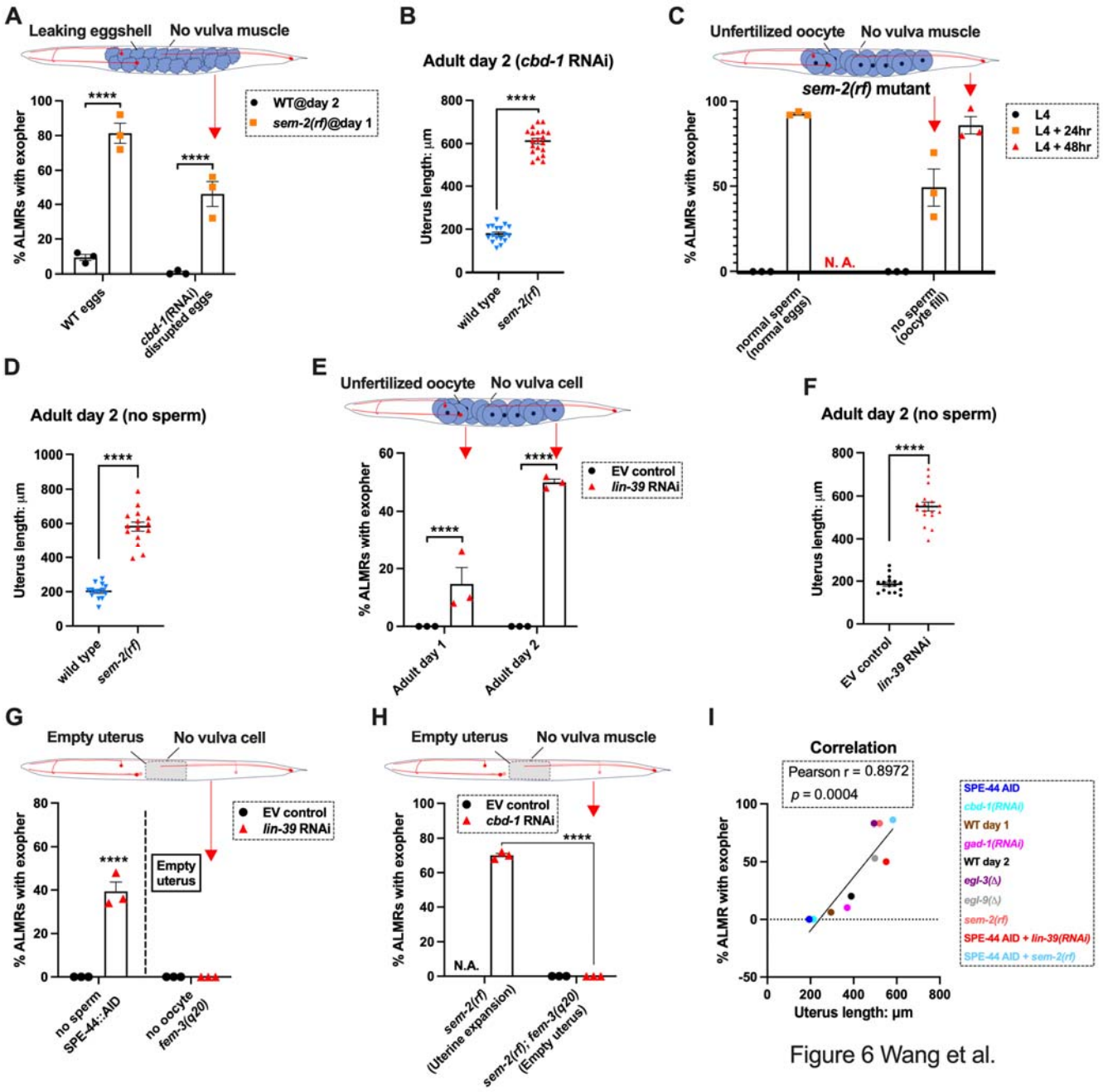

Figure 6. Uterine expansion correleates strongly with ALMR exophergenesis regardless of whether eggs, oocytes, or debris are retained.

A. **Despite *cbd-1(RNAi)* mediated disruption of eggshell formation and earliest embryonic cell divisions, exopher levels are high in the *sem-2(rf)* egg retention background.** The percentage of ALMR exopher events among 50 Ad2 wild type (left) or Ad1 *sem-2(rf)* hermaphrodite *C. elegans* that are treated with either empty vector control RNAi or RNAi targeting *cbd-1* in each trial (total of 3 independent trials). *sem-2* mutants bag extensively at Ad2 and cannot be tested. Cartoon indicates uterine filling status of test *sem-2(rf); cbd-1(RNAi)*. Strain ZB4757: bzIs166[P_{mec-4}::mCherry] II vs. strain ZB4902: *sem-2(n1343)* I; bzIs166[P_{mec-4}::mCherry] II. **** $p < 0.0001$ in Cochran–Mantel–Haenszel test.

B. **Uterine length remains long in the egg-laying defective *sem-2(rf) + cbd-1(RNAi)*.** Uterus length of strain ZB4757: bzIs166[P_{mec-4}::mCherry] II vs. ZB4902: *sem-2(n1343)* I; bzIs166[P_{mec-}

$_4$::mCherry] II treated with RNAi against *cbd-1*. n = ~20 hermaphrodites from one trial, Ad2, **** $p < 0.0001$ in two-tail unpaired *t*-test.

C. **Blocking sperm maturation in a *sem-2(rf)* mutant, which fills the uterine space with oocytes, induces exophers in the absence of eggs.** The percentage of ALMR exopher events among 50 *sem-2(rf)* hermaphrodite *C. elegans* that express the SPE-44 AID system ("control" is treated with 0.25% ethanol vehicle and "no sperm" is treated with 1mM auxin in 0.25% ethanol from egg to adult day 2) in each trial (total of 3 independent trials). L4 stage is the last larval stage before adult. Cartoon indicates uterine oocyte filling status of test *sem-2(rf); spe-44 AID*. Strain ZB4953: *sem-2(n1343)* fxIs1[P_{pie-1}::TIR1::mRuby] I; bzIs166[P_{mec-4}::mCherry] II; *spe-44(fx110[spe-44::degron]*) IV.

D. **When sperm maturation is disrupted in mutants blocked for egg laying, leaving oocytes to occupy reproductive structures, the uterus expands as oocytes accumulate**. Uterus length of strain ZB4749: fxIs1[P_{pie-1}::TIR1::mRuby] zdIs5[P_{mec-4}::GFP] I; bzIs166[P_{mec-4}::mCherry1] II; *spe-44(fx110[spe-44::degron]*) IV vs. ZB4953: *sem-2(n1343)* fxIs1[P_{pie-1}::TIR1::mRuby] I; bzIs166[P_{mec-4}::mCherry] II; *spe-44(fx110[spe-44::degron]*) IV. 1 mM auxin treatment induces the no sperm status to both strains. n = ~20 hermaphrodites from one trial, Ad2. **** $p < 0.0001$ in two-tail unpaired *t*-test.

E. **Disrupting sperm maturation in *lin-39(RNAi)* animals blocked for egg-laying fills the uterine space with oocytes, and induces exophers in the absence of eggs.** The percentage of ALMR exopher events among 50 adult day 1 or 2 SPE-44 AID no sperm hermaphrodite *C. elegans* treated with either control RNAi or *lin-39* RNAi in each trial (total of 3 independent trials). Cartoon indicates uterine oocyte filling status of test *lin-39(RNAi); spe-44 AID*. ZB4749: fxIs1[P_{pie-1}::TIR1::mRuby] zdIs5[P_{mec-4}::GFP] I; bzIs166[P_{mec-4}::mCherry1] II; *spe-44(fx110[spe-44::degron]*) IV. **** $p < 0.0001$ in Cochran–Mantel–Haenszel test.

F. **When sperm maturation is blocked, leaving oocytes to occupy reproductive structures, the uterus length is short; but if oocytes cannot be laid in the *lin-39(RNAi)* background, the uterus expands as oocytes accumulate**. Uterus length of strain ZB4749: fxIs1[P_{pie-1}::TIR1::mRuby] zdIs5[P_{mec-4}::GFP] I; bzIs166[P_{mec-4}::mCherry1] II; *spe-44(fx110[spe-44::degron]*) IV + 1 mM auxin treatment to eliminate sperm maturation. n = ~20 hermaphrodites. **** $p < 0.0001$ in two-tail unpaired *t*-test.

G. **Blocking oocyte production in the background of *lin-39(RNAi)*-mediated disruption of the egg-laying apparatus eliminates early adult exophergenesis**. We used *spe-44* AID to block sperm maturation and *fem-3(q20)* to prevent oocyte production; *lin-39(RNAi*) to disrupt egg-laying capacity. Cartoon indicates empty uterus status of test *fem-3(q20); spe-44 AID; lin-39(RNAi)* strain. Exopher scoring of Ad2 ZB4749: fxIs1[P_{pie-1}::TIR1::mRuby] zdIs5[P_{mec-4}::GFP] I; bzIs166[P_{mec-4}::mCherry1] II; *spe-44(fx110[spe-44::degron]*) IV + 1mM auxin or ZB5042: bzIs166[P_{mec-4}::mCherry] II; *fem-3(q20)ts* IV, treated with either control empty vector (EV) RNAi or *lin-39* RNAi at 25°C. Total of three trials (50 worms per trial). **** $p < 0.0001$ in Cochran–Mantel–Haenszel test.

H. **Blocking oocyte production in the background of *sem-2(rf)*-mediated disruption of the egg-laying apparatus eliminates early adult exophergenesis**. We used *cbd-1(RNAi)* to disrupt eggshell and *fem-3(q20)* to prevent oocyte production; *sem-2(n1343)* to disrupt egg-laying capacity. Exopher scoring of adult day 2 hermaphrodites, treated with either control empty vector (EV) RNAi or *cbd-1* RNAi at 25°C. Total of three trials (50 worms per trial). Cartoon indicates empty uterus status of test *fem-3(q20); cbd-1(RNAi); sem-2(rf)* strain.

I. **The uterus length is correlated with ALMR exophergenesis.** Data shown are the mean of uterus length (X aixs) and percentage ALMRs with exopher (Y axis) for different genotypes/treatments measured in this study. The correlation line is based a linear fit model and

the Pearson r and *p* value is based on the correlation assay. Uterus length from short to long: SPE-44::AID; *cbd-1(RNAi)*; wild type (adult day 1); *gad-1(RNAi)*; wild type (adult day 2); *egl-3(Δ); egl-9(Δ); sem-2(rf);* SPE-44::AID + *lin-39(RNAi);* SPE-44::AID + *sem-2(rf)*.

Sustained physical distortion of the gonad by fluid injection can rapidly elevate exopher production. To independently test for a role for physical stretch/filling of the uterus in exopher induction, we distorted the gonad compartment by injecting dye-containing M9 buffer into a very young adult. The animal subjects we tested were vulva-less *(lin-39(RNAi))* and also subjected to *spe-44* AID to block sperm production. These vulva-less + sperm-less hermaphrodites normally exhibit high ALMR exophergenesis at late Ad1 and Ad2 (Fig. 6C&D) due to oocyte accumulation. To avoid oocyte influence, we conducted our physical expansion studies just as animals reach Ad1, a time when ALMR exophergenesis is typically not observed (Fig. 7A).

We picked the L4 stage vulva-less (*lin-39(RNAi)*) + sperm-less (SPE-44 AID) hermaphrodites for age synchronization (20°C, grown for 12 hours after L4 selection) and then injected dye containing M9 buffer into the uteri of these very young adult day 1 hermaphrodites, scoring for exopher production 10 minutes after the injection (Fig. 7B).

Control animals (mock injected animals that were stabbed without fluid delivery) exhibited no ALMR exophers. By contrast, we found that when we held injection pressure continuous for 2 or more minutes, ~20% of the ALMs scored exhibited an exopher event shortly after injection (Fig. 7C&D). Injection experiments using animals with functional vulvae (in which injected material is rapidly extruded through the vulval opening) failed to induce ALMR exophers (Fig. 7E), supporting that ALMR exophergenesis caused by 2-minute injection of dye-containing M9 is due to the physical distortion of gonad rather than the chemical impact of the dye-containing M9.

In sum, exopher induction by uterine accumulation of eggs, malformed eggs, dead embryos, oocytes, or fluid-induced expansion support a model in which early adult ALMR exophergenesis is elevated by physical distortion of the uterus that occurs with reproduction (Fig. 7F).

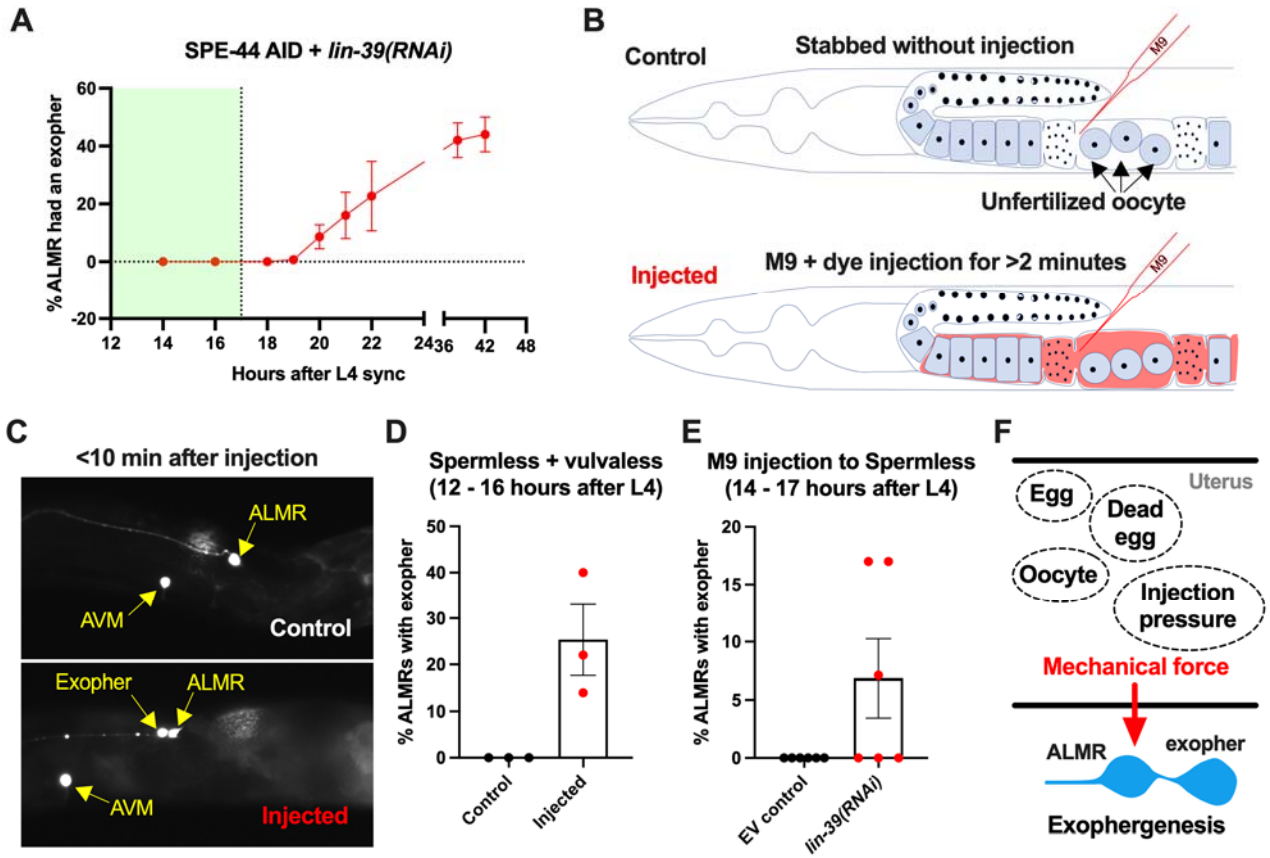

Figure 7 Wang et al.

Figure 7. ALMR exophergenesis can be induced by uterine compartment distortion that accompanies fluid injection

A. **Summary of timing of ALMR exophergenesis from age synchronized spermless + vulvaless hermaphrodite.** Total of three trials and 50 hermaphrodites in each trial. Strain ZB4749: fxIs1[P_{pie-1}::TIR1::mRuby] zdIs5[P_{mec-4}::GFP] I; bzIs166[P_{mec-4}::mCherry1] II; *spe-44(fx110[spe-44::degron])* IV, cultured on the 1 mM auxin treated NGM agar plates seeded with HT115 *E. coli* expressing dsRNA against the *C. elegans lin-39* gene. Eventually, oocytes accumulate in this strain, but at worst very few are evident in the timeframe in which we performed injections. Data shown are mean ± SEM at each time point. The data demonstrate that there is no ALMR exophergenesis in this background before the 18th hour after L4 sync. Testing the impact of injection on ALMR exophergenesis before the 17th hour after L4 thus monitors injection consequences during a timeframe in which no exophers are normally produced.

B. **Illustrated experimental design for testing the ALMR exophergenesis response to physically expanding the gonad via 2 minute continuous fluid injection.** We performed 2+ minute duration injections of M9 buffer mixed with food color dye 1:10 or 1.5:10 dye/M9 ratio (to verify successful injection; dye contains water, propylene glycol, FD&C reds 40 and 3, propylparaben) into the uteri of sperm-less only (EV control) or sperm-less + vulvaless (treated with *lin-39* RNAi) animals. Strain: ZB4749 as in panel A, treated with either empty vector (EV) or RNAi against *lin-39* in the presence of 1 mM auxin. *lin-39(RNAi)* disrupts vulval development such that injected fluids are retained to expand the uterus. In injections with animals that have functioning egg laying apparati, fluids can exit the animal and do not expand the uterus.

C. **2 minute sustained injection into egg-laying blocked, reproduction blocked animals can induce rapid exophergenesis**: representative picture of an ALMR exophergenesis event consequent to injection.

D. **2 minute sustained injection into egg-laying blocked, reproduction blocked animals can induce rapid exophergenesis**: exopher scoring of the control mock injected and 2 minute injected animals. Strain ZB4749: fxIs1[P_{pie-1}::TIR1::mRuby] zdIs5[P_{mec-4}::GFP] I; bzIs166[P_{mec-4}::mCherry1] II; *spe-44(fx110[spe-44::degron]*) IV treated with auxin and *lin-39(RNAi)* to induce the sperm-less and vulva-less status, respectively. Data represent a total of three trials (6 to 10 worms in each trial). $p < 0.05$ in Cochran–Mantel–Haenszel test, as compared to the no-injection fluid control.

E. **2 minute sustained injection induces rapid ALMR exophergenesis only from vulvaless animals**. Data showing the exopher scoring of the sperm-less EV control (with functional vulva) or sperm-less + vulvaless (treated with *lin-39* RNAi) worms. Strain: ZB4749 (genotype in panel A legend) treated with either empty vector (EV) or RNAi against *lin-39* in the presence of 1 mM auxin to disrupt sperm maturation. Data represent a total of 6 trials (6 to 10 worms in each trial). 3 out of 6 trials showed ALMR exopher induction by M9 injection to the vulvaless worms; while not a single trial produced ALMR exopher induction by M9 injection to animals with WT vulvae. If the vulva is intact, injected fluids are observed to leak out, consistent with the assumption that the gonads of egg-laying proficient animals will not sustain required expansion.

F. **Summary**. Eggs, dead egg accumulation, oocyte accumulation, or injection pressure all lead to ALMR exophergenesis. These varied interventions have a similar impact on the uterus, which is the uterine distortion by mechanical forces. We propose that early adult ALMR exophergenesis requires mechanical or stretch-assocated force generated by the uterine cargos.

DISCUSSION

Exopher production by proteo-stressed *C. elegans* touch neurons occurs with a striking temporal pattern that features a puzzling early adult peak of exophergenesis coincident with the period of maximal egg production. Here we report that the early exophergenesis peak is dependent on uterine occupation, which normally is conferred by fertilized egg accumulation prior to the deposition of eggs. Uterine expansion that is associated with the filling of a blocked uterus with unfertilized oocytes or by fluid alone can also induce high neuronal exopher production, supporting a model in which the physical distention associated with uterine occupancy, rather than chemical signals derived from fertilized eggs *per se*, is a required component of the signaling relay between reproduction and young adult neuronal debris elimination. Trans-tissue cross talk to the maternal nervous system thus appears accomplished via mechanical force transduction. Our findings hold implications for mechano-biology in neuronal proteostasis management.

The mechanical landscape of reproduction that influences neuronal exophergenesis. *C. elegans* reproduction features physical expansion and contraction of multiple tissue/cell types. The gonad houses the expanding germline, the spermatheca expands and retracts vigorously as each mature oocyte enters and exits. The uterus also stretches to house eggs and can contract locally as eggs transit or are expelled via action of the vulval and uterine muscles. The filled reproductive apparatus

can thus clearly exert both constitutive and sporadic pressure on surrounding tissues as it enacts its essential functions.

What is the source of the force that promotes exopher production? Elegant work on the egg laying circuit (comprising the somatic gonad, the HSN and VC neurons, and the vulval and uterine muscle) has provided evidence for mechanical signaling within the egg laying circuit that regulates initiation, promotion and termination of egg laying [31,57-59]. Working backward, exopher-promoting force seems unlikely to derive from the vulva or vulval muscle contractions, since when these cells are genetically disrupted in *lin-39(RNAi*) or in *sem-2* mutants, high levels of exophers still are generated. Changes in spermatheca volume, which expands and contracts dramatically as mature oocytes enter via valve opening/closure [60], might be sensed, but spermatheca contractions are reported to be normal in hyperactive egg laying *goa-1* [61], which is an exopher-suppressing background. Under no-sperm conditions, oocyte transit rates are lower than for fertilized eggs, and sperm-derived signals influence spermathecal valve opening [62-64], but if the egg laying apparatus is genetically compromised and oocytes accumulate in the absence of sperm, exopher levels are high, suggesting deficits in spermatheca operations or sperm signals *per se* do not drive exophergenesis. Given that, under normal reproductive conditions of egg-laying proficiency, correctly shelled eggs are required for the early peak in exopher production, a plausible hypothesis was that fertilized eggs might produce an essential diffusible factor that stimulates neuronal exopher-genesis. However, exophers can be produced abundantly in the absence of fertilized eggs when the vulva is unable to open and release uterine contents, resulting in uterine distention due to debris filling. Thus, the simplest model we envision for the reproductive cues that influence maternal neuronal exophergenesis is that a filled uterus (under normal conditions the consequence of hard-shelled eggs that occupy it) is sensed and required for the early adult peak in exopher production.

How might force be sensed and transduced? Mechanotransduction is the sensing of a mechanical signal, such as pressure or stretch, and conversion into a cellular response. Members of several ion channel families have been implicated in sensing of touch, hearing, shear stress, and pressure, including Piezo, TRP, and DEG/ENaC families [65]. These are rational candidates for mechanosensors in neurons, the uterus, or other cells that might act in a relay between the uterus and neuron. At the same time, classic mechanosensory channels have extremely rapid gating and might not be the best suited candidates for acting in the sustained and locally dynamic forces anticipated for the reproductive uterine environment.

Adhesion G-Protein Coupled Receptors, which have extracellular adhesion motifs and 7 transmembrane domains characteristic of the GPCR class (*lat-1*, *lat-2, cdh-6* in *C. elegans* [66-68]), or components of the YAP/TAZ transcriptional program [69] may integrate responses to forces transmitted via the cytoskeleton and could be considered as potential players in the required signaling. Determination of the identity of mechanotransducers and assignment of site of action to the neuron, the uterus, or an intermediate relay cell type remains for future studies. Modeling will also need to incorporate the fact that fluid injections, which required 2 minute long sustained application of the filling stimulus to induce exophers, could provoke exopher production on a rapid timeframe, typically recorded only 10 minutes after injection period. Thus the proteostressed touch neurons appear poised to eliminate contents upon mechanical stimulation.

Mechanical signaling in reproduction across species. Uterine stretch may be a more prevalent mechanism for inducing maternal nervous system response than currently appreciated. Distention of the female fly reproductive tract by egg passage through the tract (normal biology) or by artificial means (experimental fluid injection) can induce behavioral attraction of the mother to acetic acid, thought to signal a favorable food environment for offspring [70]. In this case, DEG/ENaC channel family member PPK1 expressed in a subset of mechanosensitve neurons that tile the tract and respond to contraction/distention of the tract is required. The pathway to the behavioral change remains to be determined. Uterine stretch in mammals has also be reported influence maternal behavior [71].

Why link exophers to reproduction? Turek et al. report that exophers produced by *C. elegans* muscle cells follow a similar time course of highest production at adult day 2, and demonstrated a

dependence of the temporal muscle exophergenesis pattern on eggs [72] (muscle exophers may be released to supply nutrients to developing progeny). Together with our observations, data raise the possibility that the onset of reproduction and the initial filling of the uterus triggers, or generates a 'license" for EV/exopher production across tissues. In the case of stressed touch receptor neurons that have been our focus, evidence suggests that deleterious protein aggregates and/or excess proteins and organelles are handed off to neighboring glial-like hypodermal cells for degradation [7]. Clearing the nervous system (and other organs) for optimal function might confer a selective advantage for successful maternal reproduction.

In this regard it is fascinating that the peak exopher production period is coincident with a proteostasis reconfiguration that has been well documented to accompany reproduction onset in young adult *C. elegans*. In brief, during larval development *C. elegans* exhibits high activity of HSF-1 and consequently HSF-1-dependent chaperone expression, but HSF-1 activity is turned down in adult life [54,55,73,74]. At the same time in early adult life, proteasome activity is relatively enhanced (at least as measured in the hypodermis) [75]. These measures may reflect a general proteostasis reorganization (chaperone activity, proteosome activity) that occurs in early adult life in response to reproduction [54,73]. Our observations on neuronal exophers suggests that exopher-mediated content elimination may constitute another co-regulated branch of this proteostasis reconfiguration. Importantly, the HSF-1 turn-down in young adult life is blocked by *cbd-1(RNAi)* (and additional early eggshell/development gene RNAi) [74]. Thus the presence of eggs can signal across tissues to turn-down *hsf-1* proteostasis-related activities in the mother. We speculate that this young adult reconfiguration of proteostasis might reflect a mechanism to optimize successful reproduction, possibly both fine tuning nervous system function and shifting resources balance to favor progeny as suggested by the disposable soma theory of aging proposed by Kirkwood [76].

Of note, we do not observe exophers in larval stages [3]. We speculate that young adult physiology might be temporally tweaked such that some tissues have optimized capacity to manage/degrade large aggregates and organelles at an early adult developmental "clean up" time, possibly analogous to how a town service for large garbage pick-up might be limited to particular times during the year. As exopher production appears generally beneficial for neuronal function and survival [3,77], the early life extrusion phase appears a positive feature of reproductive life. More broadly, proteome "clean up" phases may be programmed as key steps at specific transitions during development and homeostasis, for example, as occurs in the temporal lysosome activation that clears aggregate debris in *C. elegans* maturing oocytes [78] or in the maturation of adult neuronal stem cells via vimentin-dependent proteaseome activity during quiescence exit in the mouse [79].

Across species, production of exopher-like vesicles may also be enhanced by mechanical signals anchored outside of reproduction. For example, mice cardiomyocytes that are constantly under mechanical stress due to the contraction activities produce exopher-like vesicles [8]. Mouse kidney proximal tubular epithelia cells (PTEC) under constant mechanical stress due to both fluid shear stresses and absorption-associated osmotic pressure, also release exopher-like vesicles [80].

Large vesicle extrusion, mechanobiology and neurodegenerative disease. The impact of mechanical force on *in vivo* production of extracellular vesicles has not been a major focus of the EV field, although a range of studies have considered force consequences (such as fluid shear responses, stretch) in cultured cells. Overall, however, EV biogenesis and uptake appear to be markedly influenced by biomechanical force type, magnitude, and duration [81]. At the same time, the neurodegeneration field has generated myriad studies linking Alzheimer's disease susceptibility and AD pathology signatures such as extracellular accumulation of amyloid-β protein and/or intracellular accumulation of tau as outcomes of mechanical stress-based stimuli such as traumatic brain injury, arterial hypertension, and normal pressure hydrocephalus [82,83]. Mechanical stress may trigger or promote protein misfolding, aggregation, and extrusion. Examples of recent implication of mechanical stimuli in AD-related outcomes include that stretch in the brain vascular system can increase APP and B-secretase expression to increase Aβ production [84] and that microglial mechanosensing via the Piezo1 mechanotransducing channel limits progression of Aβ pathology in mouse models [85]. Our study reveals a capacity of mechanical force to influence neuronal release of large vesicles containing neurotoxic

species, inviting more serious consideration of the roles of mechanobiology in maintaining proteostasis and influencing aggregate transfer within the context of a living nervous system.

METHODS AND MATERIALS

Strains and maintenance

All strains used in this study carry the transgene bzIs166[P_{mec-4}::mCherry] to mark the six touch receptor neurons: ALMR, ALML, AVM, PVM, PLMR and PLML. The genotype of *C. elegans* strains used in this study are listed in Table 1. We maintained all *C. elegans* strains on nematode growth media (NGM) seeded with OP50-1 *Escherichia coli* in a 20°C or 15°C incubator. We kept all animals on food for at least 10 generations before using them in test.

Age synchronization

For the majority of experiments, we used a bleaching protocol or an egg-laying protocol for age synchronization, otherwise, we picked L4 animals for synchronization.

Temperature sensitive mutants

We maintained the age-synchronized temperature sensitive mutations in a 15°C incubator. For either *fem-1* or *fem-3* mutants, we directly placed the isolated eggs into a 25°C incubator in each experimental test. Since the egg-hatching of *glp-4* mutant is out of sync at 25°C, we placed the isolated eggs in a 15°C incubator for 24 hours before transferring them into the 25°C incubator for experimental tests.

Auxin inducible degradation

We dissolved auxin (indole-3-acetic acid, 98+%, A10556, Alfa Aesar) in 95% ethanol to make a 400mM stock, then we prepared a 40mM auxin solution by diluting the 400mM stock solution in M9 medium (which contains 1mM MgSO4) and applied 200ul of the 40mM solution on to the NMG-agar plate (which is 60mm in diameter and contains ~8-9g medium). We left the plate on an open bench at room temperature for one or two days to dry out the auxin solution, then seeded the plate with 200ul OP50-1 *E. coli* and waited for another two or three days before storing the plates in a 4°C environmental room. We only used the plates which had been stored in the 4°C environmental room for at least a week, so the concentration of auxin can be equilibrated into 1mM. We prepared the ethanol control plates under the same procedure, and the final concentration of ethanol in the control plates should be ~0.25%. To proceed auxin inducible degradation of SPE-44, we placed the isolated eggs on auxin treated plates or the ethanol control plates. After ~72 hours of culture in a 20°C incubator, the animal reached the age of adult day 1 and the auxin treated worms became sterile. Then we transferred the worms into a regular NGM-agar plate without auxin or ethanol.

Microscopy and image processing

We took the DIC or fluorescent pictures with a Zeiss compound microscope or spinning disc confocal microscope driven by MetaMorph software, then processed the pictures with Fiji ImageJ software.

Exopher scoring

Exopher numbers are variable between 5-30%, mostly 10-15% range, and reaching peak at adult day 2 [3]. We scored the exopher count with the protocol published in JOVE [14]. we examined at least 50 animals for each genotype or treatment with the FBS10 Fluorescence Biological Microscope (KRAMER scientific).

RNAi treatment

The NGM-agar RNAi plate contains 1mM IPTG and 25µg/ml carbenicillin. The food on top of the medium is HT115 bacteria expressing dsRNA against targeted gene or carrying an empty vector (EV, L4440) as the control. The treatment is from eggs to the last day of each test.

FUDR treatment

The concentration of FUDR (floxuridine) on NGM-agar plate is ~51mM. The treatment starts from adult day 1.

Male matting experiment

In each trial, we prepared ~2000 age synchronized adult day 1 hermaphrodites and did exopher counting for 50 worms from adult day 1 to day 3. In adult day 3, we divided the worms into three groups (~400 worms in each group, and ~100 worms per plate). Group 1 is the control worms without males. We added ~100 sterile males into group 2 and ~100 normal males into group 3 for each plate.

Electron microscopy

We prepared mCherry animals for TEM analysis by high pressure freezing and freeze substitution (HPF/FS), and followed a standard to preserve ultrastructure. After HPF in a Baltec HPM-010, we exposed animals to 1% osmium tetroxide, 0.1% uranyl acetate in acetone with 2% water added, held at −90 °C for 4 days before slowly warming back to −60 °C, −30 °C, and 0 °C, over a 2 day period. We rinsed the samples several times in cold acetone and embedded the samples into a plastic resin before curing them at high temperatures for 1–2 days. We collected serial thin sections on plastic-coated slot grids and post-stained them with 2% uranyl acetate and then with 1:10 Reynold's lead citrate, and examined with a JEOL JEM-1400 Plus electron microscope. By observing transverse sections for landmarks such as the 2nd bulb of the pharynx, it was possible to reach the vicinity of the ALM soma before collecting about 1500 serial thin transverse sections.

The microinjection experiment

Animals were mounted on coverslips with dried 2% agarose pads covered in halocarbon 700 oil. Coverslips were placed onto an Axiovert S100 TV Inverted Microscope (Carl Zeiss) and animals were injected with capillary needles filled with M9 + 10% red dye using 40 psi of pressure. Needles were pulled from borosil capillary tubing (1.0mm OD, 0.5mm ID; FHC) using a P-97 Micropipette Puller (Sutter Instrument). Puller parameters were as follows: Heat 474 (Ramp-25); Pull 90; Vel 100; Time 180.

Statistics

The exopher phenotype (+ or -) for each animal is a nominal variable, so we analyzed the exopher data by Cochran–Mantel–Haenszel test. There is no power analysis for each experiment, but each experiment has at least three independent trials.

Table 1: Strain list

Strain Name	Genotype	Index
N2	wild type	wild type
ZB4065	bzIs166[P_{mec-4}::mCherry] II	wild type
ZB4757	bzIs166[P_{mec-4}::mCherry] II (outcrossing ZB4065 to N2 for 6 times)	wild type
ZB4768	*glp-4(bn2)*^{ts} I; bzIs166[P_{mec-4}::mCherry] II	*glp-4(ts)*
ZB5042	bzIs166[P_{mec-4}::mcherry] II; *fem-3(q20)* IV	*fem-3(gf)*
ZB4915	bzIs166[P_{mec-4}::mCherry1] II; *fem-1(hc17)* IV	*fem-3(lf)*
ZB4749	fxIs1[P_{pie-1}::TIR1::mRuby] zdIs5[P_{mec-4}::GFP] I; bzIs166[P_{mec-4}::mCherry1] II; *spe-44(fx110[spe-44::degron])* IV.	SPE-44
ZB4941	bzIs166[P_{mec-4}::mCherry]; *gna-2(gk308)* I/hT2 [*bli-4(e937) let-?(q782*) qIs48[P_{myo-2}::GFP; P_{pes-10}::GFP; P_{ges-1}::GFP] (I;III)	*gna-2(Δ)*
AD295	*spe-45(tm3715)*; *him-5(e1490)*; asEx89 [*spe-45* "fosmid 1" mixture + P_{myo-3}::gfp]	*spe-45(tm3715)*
ZB4772	bzIs166[P_{mec-4}::mCherry] II; *egl-9(sa307)* V	*egl-9(Δ)*
ZB4904	bzIs166[P_{mec-4}::mCherry] II; *egl-3(gk238)* V	*egl-3(Δ)*
ZB4902	*sem-2(n1343)* I; bzIs166[P_{mec-4}::::mCherry] II	*sem-2(rf)*
ZB5352	*goa-1(n1134)* I; bzIs166[P_{mec-4}::mCherry] II	*goa-1(Δ)*
ZB5046	Ex [(pJC4) P_{mec-3}::gfp + pRF4]; bzIs166[P_{mec-4}::mCherry] II	pJC4 + *rol-6(su1006)*
ZB4942	fxIs1[P_{pie-1}::TIR1::mRuby] I; bzIs166[P_{mec-4}::mCherry] II; *spe-44*(fx110[*spe-44*::degron]) IV; pwSi93[P_{hyp7}::oxGFP::*lgg-1*]	Fig, 5A
ZB4953	*sem-2(n1343)* fxIs1[P_{pie-1}::TIR1::mRuby] I; bzIs166[P_{mec-4}::mCherry] II; *spe-44(fx110[spe-44::degron])* IV	*sem-2(rf)*
ZB5709	*sem-2(n1343)* I; bzIs166[P_{mec-4}::mCherry] II; *fem-3(q20)* IV.	*sem-2(rf); fem-3(q20)*

AUTHOR CONTRIBUTIONS

GW, RG, SS, EC, AM, AJS, DJ, SS, IM, and KCN did the experiment. GW, RG, SS, EC, AM, AJS, DHH, BDG, and MD designed the experiment. GW, RG, SS, DHH, BDG, and MD wrote the manuscript.

DECLARATION OF INTERESTS

The authors declare no competing interests.

AKNOWLEDGEMENT

We thank Dr. Andrew Singson, Dr. Amber Krauchunas, and Dr. Xue Mei for sharing reagents and providing comments in experimental design. We also thank the Caenorhabditis Genetics Center (CGC, founded by National Institutes of Health - Office of Research Infrastructure Programs (P40 OD010440)) for providing some strains. Funding sources: NIH R24 OD010943 to DHH; NIH 5R01GM135326 to BDG; NIH R37AG56510 to MD; and NIH R01AG047101 to MD and BDG.

REFERENCE

1. Peng, C., Trojanowski, J.Q., and Lee, V.M. (2020). Protein transmission in neurodegenerative disease. Nat Rev Neurol *16*, 199-212. 10.1038/s41582-020-0333-7.
2. Davis, A.A., Leyns, C.E.G., and Holtzman, D.M. (2018). Intercellular Spread of Protein Aggregates in Neurodegenerative Disease. Annu Rev Cell Dev Biol *34*, 545-568. 10.1146/annurev-cellbio-100617-062636.
3. Melentijevic, I., Toth, M.L., Arnold, M.L., Guasp, R.J., Harinath, G., Nguyen, K.C., Taub, D., Parker, J.A., Neri, C., Gabel, C.V., et al. (2017). C. elegans neurons jettison protein aggregates and mitochondria under neurotoxic stress. Nature *542*, 367-371. 10.1038/nature21362.
4. Cooper, J.F., Guasp, R.J., Arnold, M.L., Grant, B.D., and Driscoll, M. (2021). Stress increases in exopher-mediated neuronal extrusion require lipid biosynthesis, FGF, and EGF RAS/MAPK signaling. Proceedings of the National Academy of Sciences of the United States of America *118*. 10.1073/pnas.2101410118.
5. Arnold, M.L., Cooper, J., Androwski, R., Ardeshna, S., Melentijevic, I., Smart, J., Guasp, R.J., Nguyen, K.C.Q., Bai, G., Hall, D.H., et al. (2023). Intermediate filaments associate with aggresome-like structures in proteostressed C. elegans neurons and influence large vesicle extrusions as exophers. Nature communications *14*, 4450. 10.1038/s41467-023-39700-1.
6. Corsi, A.K., Wightman, B., and Chalfie, M. (2015). A Transparent window into biology: A primer on Caenorhabditis elegans. WormBook, 1-31. 10.1895/wormbook.1.177.1.
7. Wang, Y., Arnold, M.L., Smart, A.J., Wang, G., Androwski, R.J., Morera, A., Nguyen, K.C.Q., Schweinsberg, P.J., Bai, G., Cooper, J., et al. (2023). Large vesicle extrusions from C. elegans neurons are consumed and stimulated by glial-like phagocytosis activity of the neighboring cell. Elife *12*. 10.7554/eLife.82227.
8. Nicolas-Avila, J.A., Lechuga-Vieco, A.V., Esteban-Martinez, L., Sanchez-Diaz, M., Diaz-Garcia, E., Santiago, D.J., Rubio-Ponce, A., Li, J.L., Balachander, A., Quintana, J.A., et al. (2020). A Network of Macrophages Supports Mitochondrial Homeostasis in the Heart. Cell *183*, 94-109 e123. 10.1016/j.cell.2020.08.031.
9. Lampinen, R., Belaya, I., Saveleva, L., Liddell, J.R., Rait, D., Huuskonen, M.T., Giniatullina, R., Sorvari, A., Soppela, L., Mikhailov, N., et al. (2022). Neuron-astrocyte transmitophagy is altered in Alzheimer's disease. Neurobiol Dis *170*, 105753. 10.1016/j.nbd.2022.105753.
10. Davis, C.H., Kim, K.Y., Bushong, E.A., Mills, E.A., Boassa, D., Shih, T., Kinebuchi, M., Phan, S., Zhou, Y., Bihlmeyer, N.A., et al. (2014). Transcellular degradation of axonal mitochondria. Proceedings of the National Academy of Sciences of the United States of America *111*, 9633-9638. 10.1073/pnas.1404651111.
11. Nicolas-Avila, J.A., Sanchez-Diaz, M., and Hidalgo, A. (2021). Isolation of exophers from cardiomyocyte-reporter mouse strains by fluorescence-activated cell sorting. STAR Protoc *2*, 100286. 10.1016/j.xpro.2020.100286.
12. Nicolas-Avila, J.A., Pena-Couso, L., Munoz-Canoves, P., and Hidalgo, A. (2022). Macrophages, Metabolism and Heterophagy in the Heart. Circ Res *130*, 418-431. 10.1161/CIRCRESAHA.121.319812.
13. Hall, C.M., Moeendarbary, E., and Sheridan, G.K. (2021). Mechanobiology of the brain in ageing and Alzheimer's disease. Eur J Neurosci *53*, 3851-3878. 10.1111/ejn.14766.
14. Arnold, M.L., Cooper, J., Grant, B.D., and Driscoll, M. (2020). Quantitative Approaches for Scoring in vivo Neuronal Aggregate and Organelle Extrusion in Large Exopher Vesicles in C. elegans. Journal of visualized experiments : JoVE. 10.3791/61368.

15. Burnaevskiy, N., Chen, S., Mailig, M., Reynolds, A., Karanth, S., Mendenhall, A., Van Gilst, M., and Kaeberlein, M. (2018). Reactivation of RNA metabolism underlies somatic restoration after adult reproductive diapause in C. elegans. Elife *7*. 10.7554/eLife.36194.
16. Angeli, S., Klang, I., Sivapatham, R., Mark, K., Zucker, D., Bhaumik, D., Lithgow, G.J., and Andersen, J.K. (2013). A DNA synthesis inhibitor is protective against proteotoxic stressors via modulation of fertility pathways in Caenorhabditis elegans. Aging (Albany NY) *5*, 759-769. 10.18632/aging.100605.
17. Stein, K.K., and Golden, A. (2018). The C. elegans eggshell. WormBook *2018*, 1-36. 10.1895/wormbook.1.179.1.
18. Greenstein, D. (2005). Control of oocyte meiotic maturation and fertilization. WormBook, 1-12. 10.1895/wormbook.1.53.1.
19. Kim, S., Spike, C., and Greenstein, D. (2013). Control of oocyte growth and meiotic maturation in Caenorhabditis elegans. Adv Exp Med Biol *757*, 277-320. 10.1007/978-1-4614-4015-4_10.
20. Beanan, M.J., and Strome, S. (1992). Characterization of a germ-line proliferation mutation in C. elegans. Development *116*, 755-766.
21. Zanetti, S., Grinschgl, S., Meola, M., Belfiore, M., Rey, S., Bianchi, P., and Puoti, A. (2012). The sperm-oocyte switch in the C. elegans hermaphrodite is controlled through steady-state levels of the fem-3 mRNA. RNA *18*, 1385-1394. 10.1261/rna.031237.111.
22. Ellis, R., and Schedl, T. (2007). Sex determination in the germ line. WormBook, 1-13. 10.1895/wormbook.1.82.2.
23. Ahringer, J., and Kimble, J. (1991). Control of the sperm-oocyte switch in Caenorhabditis elegans hermaphrodites by the fem-3 3' untranslated region. Nature *349*, 346-348. 10.1038/349346a0.
24. Doniach, T., and Hodgkin, J. (1984). A sex-determining gene, fem-1, required for both male and hermaphrodite development in Caenorhabditis elegans. Dev Biol *106*, 223-235. 10.1016/0012-1606(84)90077-0.
25. Nishimura, K., Fukagawa, T., Takisawa, H., Kakimoto, T., and Kanemaki, M. (2009). An auxin-based degron system for the rapid depletion of proteins in nonplant cells. Nat Methods *6*, 917-922. 10.1038/nmeth.1401.
26. Zhang, L., Ward, J.D., Cheng, Z., and Dernburg, A.F. (2015). The auxin-inducible degradation (AID) system enables versatile conditional protein depletion in C. elegans. Development *142*, 4374-4384. 10.1242/dev.129635.
27. Kasimatis, K.R., Moerdyk-Schauwecker, M.J., and Phillips, P.C. (2018). Auxin-Mediated Sterility Induction System for Longevity and Mating Studies in Caenorhabditis elegans. G3 (Bethesda) *8*, 2655-2662. 10.1534/g3.118.200278.
28. Kulkarni, M., Shakes, D.C., Guevel, K., and Smith, H.E. (2012). SPE-44 implements sperm cell fate. PLoS genetics *8*, e1002678. 10.1371/journal.pgen.1002678.
29. Rose, L., and Gonczy, P. (2014). Polarity establishment, asymmetric division and segregation of fate determinants in early C. elegans embryos. WormBook, 1-43. 10.1895/wormbook.1.30.2.
30. Schneider, S.Q., and Bowerman, B. (2003). Cell polarity and the cytoskeleton in the Caenorhabditis elegans zygote. Annu Rev Genet *37*, 221-249. 10.1146/annurev.genet.37.110801.142443.
31. Medrano, E., and Collins, K.M. (2023). Muscle-directed mechanosensory feedback activates egg-laying circuit activity and behavior in Caenorhabditis elegans. Curr Biol *33*, 2330-2339 e2338. 10.1016/j.cub.2023.05.008.
32. Gonzalez, D.P., Lamb, H.V., Partida, D., Wilson, Z.T., Harrison, M.C., Prieto, J.A., Moresco, J.J., Diedrich, J.K., Yates, J.R., 3rd, and Olson, S.K. (2018). CBD-1 organizes two independent

complexes required for eggshell vitelline layer formation and egg activation in C. elegans. Dev Biol *442*, 288-300. 10.1016/j.ydbio.2018.08.005.

33. Johnston, W.L., Krizus, A., and Dennis, J.W. (2006). The eggshell is required for meiotic fidelity, polar-body extrusion and polarization of the C. elegans embryo. BMC Biol *4*, 35. 10.1186/1741-7007-4-35.

34. Olson, S.K., Greenan, G., Desai, A., Muller-Reichert, T., and Oegema, K. (2012). Hierarchical assembly of the eggshell and permeability barrier in C. elegans. J Cell Biol *198*, 731-748. 10.1083/jcb.201206008.

35. Severson, A.F., Baillie, D.L., and Bowerman, B. (2002). A Formin Homology protein and a profilin are required for cytokinesis and Arp2/3-independent assembly of cortical microfilaments in C. elegans. Curr Biol *12*, 2066-2075. 10.1016/s0960-9822(02)01355-6.

36. Rappleye, C.A., Paredez, A.R., Smith, C.W., McDonald, K.L., and Aroian, R.V. (1999). The coronin-like protein POD-1 is required for anterior-posterior axis formation and cellular architecture in the nematode caenorhabditis elegans. Genes Dev *13*, 2838-2851. 10.1101/gad.13.21.2838.

37. Rappleye, C.A., Tagawa, A., Le Bot, N., Ahringer, J., and Aroian, R.V. (2003). Involvement of fatty acid pathways and cortical interaction of the pronuclear complex in Caenorhabditis elegans embryonic polarity. BMC Dev Biol *3*, 8. 10.1186/1471-213X-3-8.

38. Benenati, G., Penkov, S., Muller-Reichert, T., Entchev, E.V., and Kurzchalia, T.V. (2009). Two cytochrome P450s in Caenorhabditis elegans are essential for the organization of eggshell, correct execution of meiosis and the polarization of embryo. Mech Dev *126*, 382-393. 10.1016/j.mod.2009.02.001.

39. Johnston, W.L., and Dennis, J.W. (2012). The eggshell in the C. elegans oocyte-to-embryo transition. Genesis *50*, 333-349. 10.1002/dvg.20823.

40. Schonegg, S., Hyman, A.A., and Wood, W.B. (2014). Timing and mechanism of the initial cue establishing handed left-right asymmetry in Caenorhabditis elegans embryos. Genesis *52*, 572-580. 10.1002/dvg.22749.

41. Luke-Glaser, S., Pintard, L., Lu, C., Mains, P.E., and Peter, M. (2005). The BTB protein MEL-26 promotes cytokinesis in C. elegans by a CUL-3-independent mechanism. Curr Biol *15*, 1605-1615. 10.1016/j.cub.2005.07.068.

42. Schierenberg, E., Miwa, J., and von Ehrenstein, G. (1980). Cell lineages and developmental defects of temperature-sensitive embryonic arrest mutants in Caenorhabditis elegans. Dev Biol *76*, 141-159. 10.1016/0012-1606(80)90368-1.

43. Trent, C., Tsuing, N., and Horvitz, H.R. (1983). Egg-laying defective mutants of the nematode Caenorhabditis elegans. Genetics *104*, 619-647. 10.1093/genetics/104.4.619.

44. Salem, J.B., Nkambeu, B., Arvanitis, D.N., and Beaudry, F. (2018). Deciphering the Role of EGL-3 for Neuropeptides Processing in Caenorhabditis elegans Using High-Resolution Quadrupole-Orbitrap Mass Spectrometry. Neurochem Res *43*, 2121-2131. 10.1007/s11064-018-2636-2.

45. Wagmaister, J.A., Gleason, J.E., and Eisenmann, D.M. (2006). Transcriptional upregulation of the C. elegans Hox gene lin-39 during vulval cell fate specification. Mech Dev *123*, 135-150. 10.1016/j.mod.2005.11.003.

46. Sternberg, P.W. (2005). Vulval development. WormBook, 1-28. 10.1895/wormbook.1.6.1.

47. Chase, D.L., and Koelle, M.R. (2007). Biogenic amine neurotransmitters in C. elegans. WormBook, 1-15. 10.1895/wormbook.1.132.1.

48. Horvitz, H.R., Chalfie, M., Trent, C., Sulston, J.E., and Evans, P.D. (1982). Serotonin and octopamine in the nematode Caenorhabditis elegans. Science *216*, 1012-1014. 10.1126/science.6805073.

49. Waggoner, L.E., Hardaker, L.A., Golik, S., and Schafer, W.R. (2000). Effect of a neuropeptide gene on behavioral states in Caenorhabditis elegans egg-laying. Genetics *154*, 1181-1192. 10.1093/genetics/154.3.1181.
50. Chalfie, M., and Sulston, J. (1981). Developmental genetics of the mechanosensory neurons of Caenorhabditis elegans. Dev Biol *82*, 358-370. 10.1016/0012-1606(81)90459-0.
51. Goodman, M.B. (2006). Mechanosensation. WormBook, 1-14. 10.1895/wormbook.1.62.1.
52. Sym, M., Robinson, N., and Kenyon, C. (1999). MIG-13 positions migrating cells along the anteroposterior body axis of C. elegans. Cell *98*, 25-36. 10.1016/S0092-8674(00)80603-0.
53. Toms, N., Cooper, J., Patchen, B., and Aamodt, E. (2001). High copy arrays containing a sequence upstream of mec-3 alter cell migration and axonal morphology in C. elegans. BMC Dev Biol *1*, 2. 10.1186/1471-213x-1-2.
54. Labbadia, J., and Morimoto, R.I. (2014). Proteostasis and longevity: when does aging really begin? F1000Prime Rep *6*, 7. 10.12703/P6-7.
55. Labbadia, J., and Morimoto, R.I. (2015). Repression of the Heat Shock Response Is a Programmed Event at the Onset of Reproduction. Mol Cell *59*, 639-650. 10.1016/j.molcel.2015.06.027.
56. Johnston, W.L., Krizus, A., and Dennis, J.W. (2010). Eggshell chitin and chitin-interacting proteins prevent polyspermy in C. elegans. Curr Biol *20*, 1932-1937. 10.1016/j.cub.2010.09.059.
57. Ravi, B., Garcia, J., and Collins, K.M. (2018). Homeostatic Feedback Modulates the Development of Two-State Patterned Activity in a Model Serotonin Motor Circuit in Caenorhabditis elegans. The Journal of neuroscience : the official journal of the Society for Neuroscience *38*, 6283-6298. 10.1523/JNEUROSCI.3658-17.2018.
58. Kopchock, R.J., 3rd, Ravi, B., Bode, A., and Collins, K.M. (2021). The Sex-Specific VC Neurons Are Mechanically Activated Motor Neurons That Facilitate Serotonin-Induced Egg Laying in C. elegans. The Journal of neuroscience : the official journal of the Society for Neuroscience *41*, 3635-3650. 10.1523/JNEUROSCI.2150-20.2021.
59. Ravi, B., Zhao, J., Chaudhry, S.I., Signorelli, R., Bartole, M., Kopchock, R.J., Guijarro, C., Kaplan, J.M., Kang, L., and Collins, K.M. (2021). Presynaptic Galphao (GOA-1) signals to depress command neuron excitability and allow stretch-dependent modulation of egg laying in Caenorhabditis elegans. Genetics *218*. 10.1093/genetics/iyab080.
60. Tan, P.Y., and Zaidel-Bar, R. (2015). Transient membrane localization of SPV-1 drives cyclical actomyosin contractions in the C. elegans spermatheca. Curr Biol *25*, 141-151. 10.1016/j.cub.2014.11.033.
61. Govindan, J.A., Cheng, H., Harris, J.E., and Greenstein, D. (2006). Galphao/i and Galphas signaling function in parallel with the MSP/Eph receptor to control meiotic diapause in C. elegans. Curr Biol *16*, 1257-1268. 10.1016/j.cub.2006.05.020.
62. McCarter, J., Bartlett, B., Dang, T., and Schedl, T. (1999). On the control of oocyte meiotic maturation and ovulation in Caenorhabditis elegans. Dev Biol *205*, 111-128. 10.1006/dbio.1998.9109.
63. Miller, M.A., Nguyen, V.Q., Lee, M.H., Kosinski, M., Schedl, T., Caprioli, R.M., and Greenstein, D. (2001). A sperm cytoskeletal protein that signals oocyte meiotic maturation and ovulation. Science *291*, 2144-2147. 10.1126/science.1057586.
64. McGovern, M., Yu, L., Kosinski, M., Greenstein, D., and Savage-Dunn, C. (2007). A role for sperm in regulation of egg-laying in the nematode C. elegans. BMC Dev Biol *7*, 41. 10.1186/1471-213X-7-41.
65. Delmas, P., and Coste, B. (2013). Mechano-gated ion channels in sensory systems. Cell *155*, 278-284. 10.1016/j.cell.2013.09.026.

66. Mee, C.J., Tomlinson, S.R., Perestenko, P.V., De Pomerai, D., Duce, I.R., Usherwood, P.N., and Bell, D.R. (2004). Latrophilin is required for toxicity of black widow spider venom in Caenorhabditis elegans. The Biochemical journal *378*, 185-191. 10.1042/BJ20031213.
67. Willson, J., Amliwala, K., Davis, A., Cook, A., Cuttle, M.F., Kriek, N., Hopper, N.A., O'Connor, V., Harder, A., Walker, R.J., and Holden-Dye, L. (2004). Latrotoxin receptor signaling engages the UNC-13-dependent vesicle-priming pathway in C. elegans. Curr Biol *14*, 1374-1379. 10.1016/j.cub.2004.07.056.
68. Hutter, H., Vogel, B.E., Plenefisch, J.D., Norris, C.R., Proenca, R.B., Spieth, J., Guo, C., Mastwal, S., Zhu, X., Scheel, J., and Hedgecock, E.M. (2000). Conservation and novelty in the evolution of cell adhesion and extracellular matrix genes. Science *287*, 989-994. 10.1126/science.287.5455.989.
69. Panciera, T., Azzolin, L., Cordenonsi, M., and Piccolo, S. (2017). Mechanobiology of YAP and TAZ in physiology and disease. Nature reviews. Molecular cell biology *18*, 758-770. 10.1038/nrm.2017.87.
70. Gou, B., Liu, Y., Guntur, A.R., Stern, U., and Yang, C.H. (2014). Mechanosensitive neurons on the internal reproductive tract contribute to egg-laying-induced acetic acid attraction in Drosophila. Cell Rep *9*, 522-530. 10.1016/j.celrep.2014.09.033.
71. Kristal, M.B. (2009). The biopsychology of maternal behavior in nonhuman mammals. ILAR J *50*, 51-63. 10.1093/ilar.50.1.51.
72. Turek, M., Banasiak, K., Piechota, M., Shanmugam, N., Macias, M., Sliwinska, M.A., Niklewicz, M., Kowalski, K., Nowak, N., Chacinska, A., and Pokrzywa, W. (2021). Muscle-derived exophers promote reproductive fitness. EMBO Rep *22*, e52071. 10.15252/embr.202052071.
73. Sala, A.J., and Morimoto, R.I. (2022). Protecting the future: balancing proteostasis for reproduction. Trends in cell biology *32*, 202-215. 10.1016/j.tcb.2021.09.009.
74. Sala, A.J., Bott, L.C., Brielmann, R.M., and Morimoto, R.I. (2020). Embryo integrity regulates maternal proteostasis and stress resilience. Genes Dev *34*, 678-687. 10.1101/gad.335422.119.
75. Liu, G., Rogers, J., Murphy, C.T., and Rongo, C. (2011). EGF signalling activates the ubiquitin proteasome system to modulate C. elegans lifespan. EMBO J *30*, 2990-3003. 10.1038/emboj.2011.195.
76. Kirkwood, T.B., and Holliday, R. (1979). The evolution of ageing and longevity. Proc R Soc Lond B Biol Sci *205*, 531-546. 10.1098/rspb.1979.0083.
77. Yang, Y., Arnold, M.L., Choy, E.H., Lange, C.M., Poon, K., Broussalian, M., Sun, L.-H., Moreno, T.M., Singh, A., Driscoll, M., et al. (2022). Inhibition of early-acting autophagy genes in C. elegans neurons improves protein homeostasis, promotes exopher production, and extends lifespan via the ATG-16.2 WD40 domain. bioRxiv, 2022.2012.2012.520171. 10.1101/2022.12.12.520171.
78. Bohnert, K.A., and Kenyon, C. (2017). A lysosomal switch triggers proteostasis renewal in the immortal C. elegans germ lineage. Nature *551*, 629-633. 10.1038/nature24620.
79. Morrow, C.S., Porter, T.J., Xu, N., Arndt, Z.P., Ako-Asare, K., Heo, H.J., Thompson, E.A.N., and Moore, D.L. (2020). Vimentin Coordinates Protein Turnover at the Aggresome during Neural Stem Cell Quiescence Exit. Cell Stem Cell *26*, 558-568.e559. 10.1016/j.stem.2020.01.018.
80. Huang, Y., Yu, M., and Zheng, J. (2023). Proximal tubules eliminate endocytosed gold nanoparticles through an organelle-extrusion-mediated self-renewal mechanism. Nat Nanotechnol. 10.1038/s41565-023-01366-7.
81. Thompson, W., and Papoutsakis, E.T. (2023). The role of biomechanical stress in extracellular vesicle formation, composition and activity. Biotechnol Adv *66*, 108158. 10.1016/j.biotechadv.2023.108158.

82. Ramos-Cejudo, J., Wisniewski, T., Marmar, C., Zetterberg, H., Blennow, K., de Leon, M.J., and Fossati, S. (2018). Traumatic Brain Injury and Alzheimer's Disease: The Cerebrovascular Link. EBioMedicine *28*, 21-30. 10.1016/j.ebiom.2018.01.021.
83. Malone, J.E., Elkasaby, M.I., and Lerner, A.J. (2022). Effects of Hypertension on Alzheimer's Disease and Related Disorders. Curr Hypertens Rep *24*, 615-625. 10.1007/s11906-022-01221-5.
84. Gangoda, S.V.S., Avadhanam, B., Jufri, N.F., Sohn, E.H., Butlin, M., Gupta, V., Chung, R., and Avolio, A.P. (2018). Pulsatile stretch as a novel modulator of amyloid precursor protein processing and associated inflammatory markers in human cerebral endothelial cells. Sci Rep *8*, 1689. 10.1038/s41598-018-20117-6.
85. Hu, J., Chen, Q., Zhu, H., Hou, L., Liu, W., Yang, Q., Shen, H., Chai, G., Zhang, B., Chen, S., et al. (2023). Microglial Piezo1 senses Abeta fibril stiffness to restrict Alzheimer's disease. Neuron *111*, 15-29 e18. 10.1016/j.neuron.2022.10.021.